A Publication for the
Radio Amateur Worldwide

Especially Covering VHF,
UHF and Microwaves

VHF
COMMUNICATIONS

Volume No. 24 . Summer . 2/1992 . £3.50

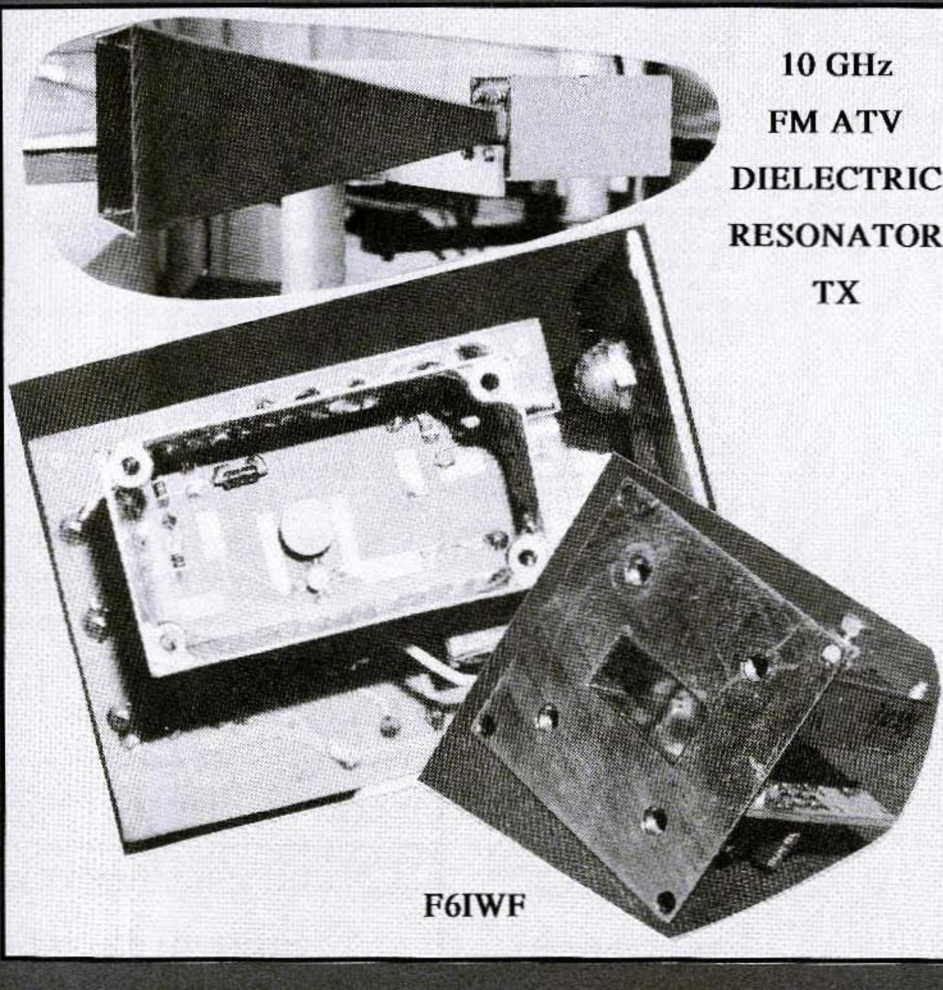

10 GHz
FM ATV
DIELECTRIC
RESONATOR
TX

F6IWF

VHF COMMUNICATIONS

A Publication for the Radio Amateur Worldwide

Especially Covering VHF, UHF and Microwaves

Volume No. 24 . Summer . Edition 2/1992

Published by: KM PUBLICATIONS,
5 Ware Orchard, Barby, Nr. Rugby,
CV23 8UF, United Kingdom.

Publishers: KM PUBLICATIONS

Editors: Mike Wooding G6IQM
Kim Wooding

Advertising Manager: Mike Wooding G6IQM

VHF COMMUNICATIONS

The international edition of the German publication UKW-BERICHTE is a quarterly amateur radio magazine especially catering for the VHF/UHF/SHF technology. It is published in Spring, Summer, Autumn and Winter under licence in the United Kingdom by KM PUBLICATIONS.

The 1992 subscription price is £12.00, or national equivalent per year. Individual copies are available at £3.50, or national equivalent each. Subscriptions, orders of individual copies, advertisements and contributions to the magazine should be addressed to the national representative, or - if not possible - directly to the publishers.

Back copies, kits, as well as the blue plastic binders are obtainable from your national representative or from KM Publications in the U.K.

Translated by Inter-Ling Services Ltd., 16 Naseby Road, Rugby, CV22 5NH, U.K.

Printed in the United Kingdom by: Apex Printers, 1 Avon Industrial Estate, Butlers Leap, Rugby, CV21 3UY.

Please address your orders or enquiries to your representative.

REPRESENTATIVES:

A U S T R I A - Verlag UKW-BERICHTE, Terry D. Bittan, POB 80, D-8523 Baiersdorf, West Germany. Telephone: (9133) 47-0. Telex: 629 887. Postgiro Nbg: 30455-858. Fax: 09733 4747.

A U S T R A L I A - W.I.A., P.O. Box 300, South Caulfield, 3162 VIC, Australia. Telephone: 5285962.

B E L G I U M - UKW.Berichte, P.O. Box 80, D-8523 Baiersdorf, West Germany. Tel: 09133-47-0. Postgiro: Nbg. 30455-858. Fax: 09133-4747.

D E N M A R K - HALSKOV ELECTRONIC OZ7LX, Sigersted gamle Skole, DK-4100 RINGSTED, Denmark. Telephone: 53-616162 (kl.19-22). Giro: 7 29 68 00.

F R A N C E - Christianne Michèl F5SM, SM ELECTRONIC, 20 bis, Avenue des Clarions, F-89000 AUXERRE, France. Telephone: (86) 46 96 59.

F I N L A N D - Peter Lytz OH2AVP, Ylākartanonkuja 5 A 9, SF-02360 ESPOO, Finland.

SRAT, PL 44, SF-00441 HELSINKI, Finland. Telephone: 358/0/5625973.

G E R M A N Y - UKW.Berichte, P.O. Box 80, D-8523 Baiersdorf, West Germany. Tel: 09133-47-0. Postgiro: Nbg. 30455-858. Fax: 09133-4747.

G R E E C E - C+A ELECTRONIC, P.O. Box 25070, Athens 100 26, Greece. Telephone: 01 52 42 867. Fax: 01 52 42 537

H O L L A N D - KM PUBLICATIONS, 5 Ware Orchard, Barby, Nr. Rugby, CV23 8UF, U.K. Telephone: 0788 890365.

I S R A E L - Doron Jacobi 4Z4RG, P.O. Box 6382, HAIFA, Israel 31063.

I T A L Y - ADB ELETTRONICA di Lucchesi Fabrizio IW5ADB, Via del Cantone 714, 55100 ANTRACCOLI (LUCCA), Italy. Telephone: 0583-952612.

L U X E M B O U R G - TELECO, Jos. Faber LX1DE, 5-9 Rue de la Fontaine, ESCH-SUR-ALZETTE, Luxembourg.

N E W Z E A L A N D - E.M.Zimmerman ZL1AGQ, P.O.Box 31-261, Milford, AUCKLAND 9, New Zealand. Telephone: (9) 486 2744.

N O R W A Y - HENNING THEG RADIO COMMUNICATION LA4YG, Kjøiaveien 30, 1370, ASKER, Norway. Postgirokonto: 3 16 00 09.

S O U T H A F R I C A - HI-TECH BOOKS, P.O.Box 1142, RANDBURG Transvaal 2125, South Africa. Telephone: (011) 886-2020.

S P A I N & P O R T U G A L - Julio A. Prieto Alonso EA4CJ, MADRID-15, Donoso Cortès 58 5°-B, Spain. Telephone: 543.83.84.

S W E D E N - Lars Petterson SM4IVE, Pl. 1254, Smégården Talby, S-17500 ODENSBACKEN, Sweden. Telephone: 19-50223. Postgiro: 914379-3.

S W I T Z E R L A N D - Terry Bittan. PSchKto. ZÜRICH 80-54.849-8.

U N I T E D K I N G D O M - KM PUBLICATIONS, 5 Ware Orchard, Barby, Nr. Rugby, CV23 8UF. Telephone: 0788 890365 & 0788 561281. FAX: 0788 890365

U S A - WYMAN RESEARCH INC., RR#1 Box 95, Waldron, Indiana 46182, USA. Telephone: (317) 525-6452.
HENRY RUH, ATVQ MAGAZINE, 1545 Lee Street, Suite 73, Des Plaines, IL. 60018, USA. Tel: (708) 298 2269. FAX: (708) 291 1644.

ISSN 0177-7505

Contents

KM Publications, 5 Ware Orchard, Barby, Nr. Rugby, CV23 8UF, U.K.

Telephone: U.K: 0788 890365; INT: + 44 788 890365. FAX: 0788 890365

Denys Roussel F6IWF

A 10 GHz FM Television Transmitter Stabilised by a Dielectric Resonator

To transmit television pictures on 10 GHz, radio amateurs generally use Gunn diode oscillator cavities, knowing the disadvantages (low efficiency, small RF power, frequency drift). However, a MeSFET transistor oscillator, stabilised by a dielectric resonator, exhibits an efficiency of about 20%, against 1 to 2% for a Gunn unit, and a stability about 20 times better. If you add to this a respectable power output of 30 to 40 mW and a good quality modulating stage, you will not need much more convincing of the viability of this simple to construct and reproducible design.

1. Circuit Description

The circuit diagram of the oscillator is shown in Fig.1. The oscillator is built around a dielectric resonator, which is a ceramic cylinder that works as a resonant circuit with a quality factor of about 5000 at 10 GHz, which is similar to that of a crystal at frequencies below 100 MHz.

In a strip line circuit, the resonator is placed close to the lines, the coupling being essentially inductive. Frequency tuning is achieved by adjusting the position of a metal disc above the resonator. Taking a closer look at the resonant circuit (Fig.2): the two lines L1 and L2 split up into l1, l2, l3, l4, with mutual inductive coupling with the dielectric resonator. Oscillation only occurs at the resonant frequency of the dielectric part. The line L3 and the strip-line capacitor C3 match the oscillator output to the antenna.

Frequency modulation is difficult to achieve, especially in wide-band FM television, which requires of the order of at least 8 MHz deviation. Because of the price and poor availability of microwave varactor diodes, tests were made to try and use the internal

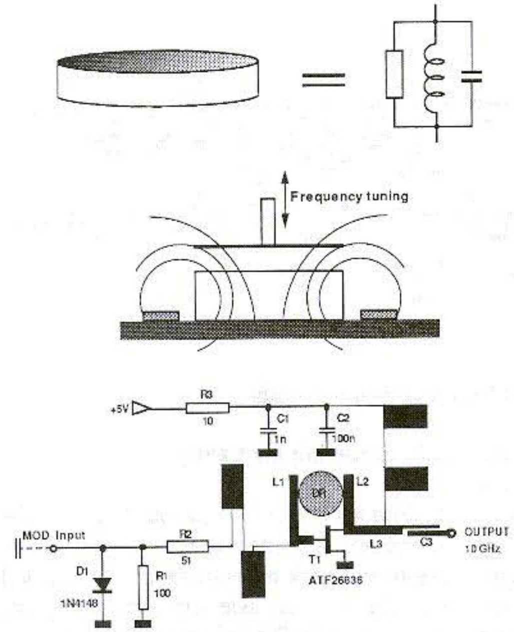

Fig.1: Circuit Diagram of the oscillator

transistor capacity change, produced by the voltage change between gate and source of a field effect transistor. More than 20 different types of transistor from different manufacturers were tried, and finally the ATF268336 from AVANTEK was chosen for its modulation characteristics using the above method. This device is a MeSFET transistor housed in a ceramic package intended for satellite low noise converters; it was designed to work up to 16GHz and is readily available at a reasonable price.

The modulating signal is applied to the transistor gate, in parallel with an 1N4148 diode and a 100 ohm resistor. The diode prevents the voltage from becoming positive, whilst the low value of R1 limits parasitic voltages, even if it is necessary to increase the value of the video link capacitor and put an additional stage in the modulator. The modulator circuit shown in Fig.3 is very simple: the input base-band video signal is first applied to a CCIR 405 pre-emphasis stage, the output of which is fed to an inverting amplifier T1, followed by an impedance matching stage T2.

The printed circuit board is made in two parts and it is thus possible to cut the board in order to remove the pre-emphasis circuit if the unit is to be used for for high speed data transmissions.

The modulation applied to the MeSFET gate is negative-going in order to obtain the conventional deviation sense, i.e: the frequency increases when the voltage at the modulation input increases.

The oscillator circuit is also powered from the supply circuit shown in Fig.3. D1 offers protection against polarity inversions and C4

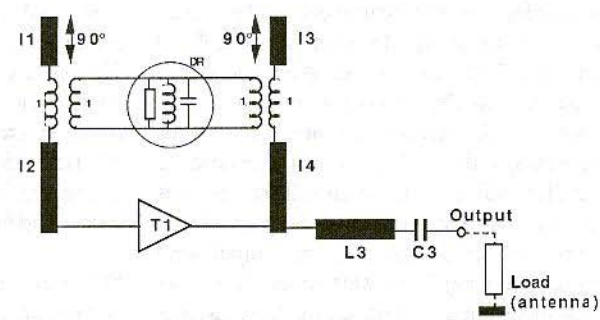

Fig.2: Theoretical circuit of the Dielectric Resonator and the Strip Line Inductors

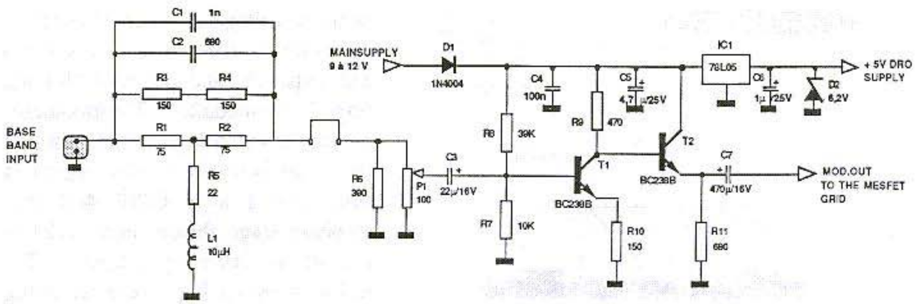

Fig.3: Circuit Diagram of the Modulator and Power Supply

and C5 are conventional bypassing capacitors. IC1 stabilises voltage at 5V and D2 provides a safety limit of 6.2V, thus cutting all spikes, which could destruct the oscillator transistor. To increase the power a little bit, IC1 could possibly be replaced by a 78L06 regulator and D2 by a 6.8V Zener diode, but this is not advised as the transistor has a rated maximum of 7V between Drain and Source.

2. CONSTRUCTION

2.1 Mechanical Design

The mechanical section (Fig.4) is made up of a shielded printed circuit block soldered onto a waveguide cavity, closed off at one end and with a WR75 flange at the other. The WR75 standard was chosen because it is the flange used on all satellite low-noise converters operating in the Ku band. It is usable down to 10 GHz, which is the low cut-off frequency of this size of waveguide. The waveguide flange allows direct coupling to the output feed whilst ensuring it is waterproof. It is also recommended that if the unit is to be used in portable locations, then a housing fabricated from, say, epoxy-glass PCB material should be constructed to cover the module.

2.2 Preparing the Cavity

Referring to figure 4: cut out and fold the waveguide and solder it edge to edge. Next, centre and mark the antenna access hole and drill the soldered side while protecting the inside of guide. Cut and drill the input flange, fit the flange over the waveguide and solder in place. The waveguide and flange should form a flush surface. Solder in place the closed-end flange fixing nuts, ensuring that the solder joints are waterproof. This will ensure that the complete assembly is weatherproof for portable use.

2.3 The Printed Circuit Block

Print and carefully etch the Teflon-glass printed circuit board from the layout shown in Fig.5 (actual size 22 x 40mm). Silver-plate the copper on both two sides. Drill 1.3mm diameter ground pin holes for the transistor T1. Drill 0.8mm ground pin holes around the circuit and holes for the entry of the +5 volt supply and the modulating signal.

Solder the ground pins of the transistor on the copper side (Silver-plated wire 1.2mm diameter). On the print side, cut short the transistor ground pins and file them down to 0.2 to 0.4mm above the PCB surface. Be careful to

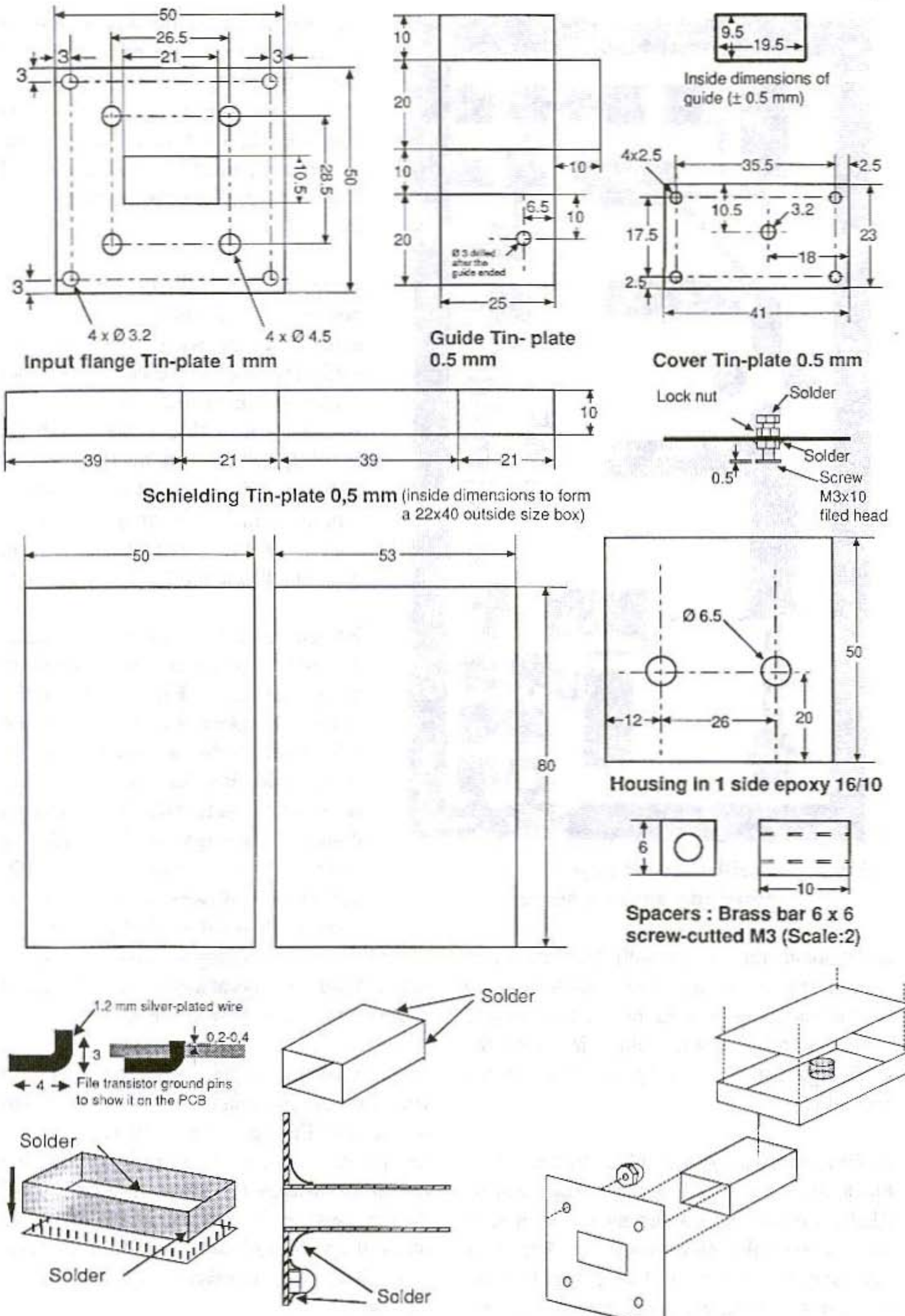

Fig.4: Mechanical Dimensions

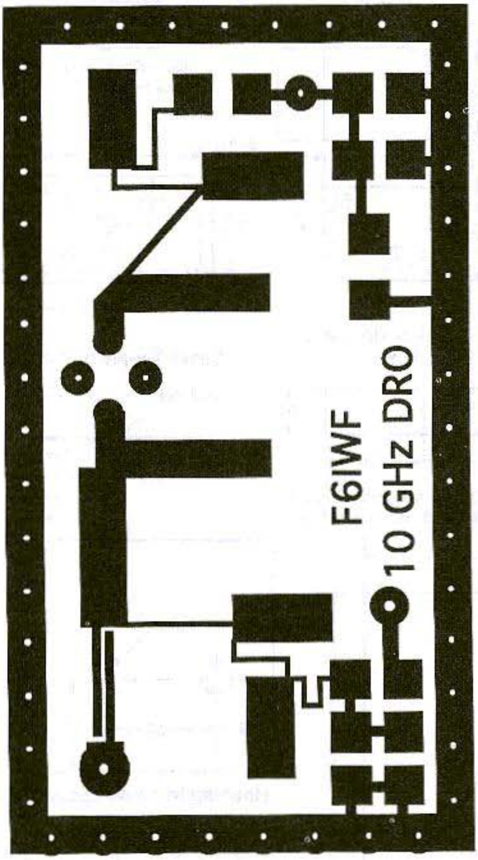

Fig.5: Oscillator PCB Layout
Finished size: 22 x 40mm

not damage the circuit with the file! Place around the circuit board and solder on the ground side the ground pins (Silver-plated wire 0.8mm). Fit and solder in place the shielding, which must be soldered to the ground pins.

Position the waveguide unit onto the circuit block and note which ground pins must be filed away on the ground side (the area in contact with the guide must be flat). It is necessary to keep 0.2 to 0.3mm length of pin remaining to ensure a good electrical contact between the two PCB sides. With a 4mm drill remove the copper around the antenna access hole on the ground side. Solder the transmitting antenna perpendicularly to the printed circuit block as shown in Fig.6 and cut to exactly 5mm up from the circuit. The antenna end must be flat, if necessary finish with file.

Place the cavity in position over the printed circuit block, centre the antenna in the waveguide hole and solder the block to the waveguide. The solder infiltrates between the guide and the ground side of the circuit by capillary action and thus ensures a good ground connection and a weatherproof seal. Solder 2mm nuts in the corners of the printed circuit block, they should not overlap the shield box.

Fit and solder all the passive components referring to the component layout shown in Fig.7. Position the transistor, solder the drain, then the grid, and then the two source connections. Soldering the source connections can be quite difficult, as the heat drain is quite large, so a hot soldering temperature is required (350 to 400 degrees C). However, care must be taken not to overheat the transistor and destroy it. Gentle cooling is recommended, do not use freezer sprays at any time, as this rapid cooling can also destroy the device.

After installation the transistor can be checked with a digital multimeter: between drain and source, the FET presents a 10 to 15 ohms resistance, between grid and source the resistance measured in circuit will be that of the combination R1 and R2, in this case 150 ohms. If you find a low G-S or D-S resistance (few Ohms), the transistor may be severely damaged.

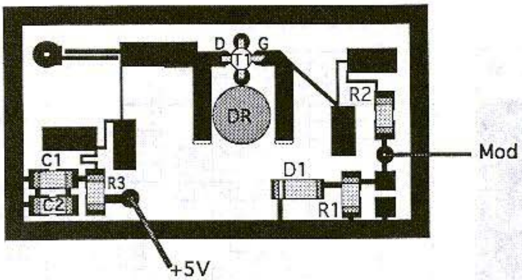

Fig.6 Component Overlay for Oscillator

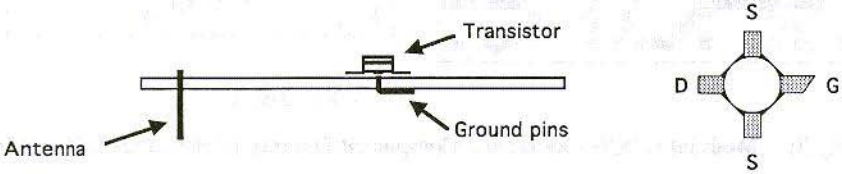

The P.C.B was optimized for segment 10.3 - 10.5 of the 10 GHz band. For lower frequencies, the lines L1, L2 must be extend by 0.5 mm (2mm on the 4:1 scale drawing) as dotted lines on the layout.

With a 4mm drill remove the copper around the power supply and modulating signal input holes on the ground side. Pass wires through the holes in the board and solder on the component side (to make the tests easier keep the supply wire 1m long).

After the modulator/power supply board has been built according to the PCB layout and component overlay shown in Fig.7. and the power supply section tested, connect the two boards together. Finally, clean the printed circuits with acetone or other solvent to remove all traces of resin-core residues.

3. TESTING AND ALIGNMENT

Warning! microwaves can cause severe and permanent damage to the human body. When you switch on a microwave source, never point the output towards anyone. Never look into a waveguide or feed when the source is switched on and radiating!

3.1 Initial setup

A 10 GHz FM television receiver and a wavemeter, microwave frequency counter or spectrum analyser are required for testing.

Transistors able to work at these frequencies are quite fragile and expensive. The solution to save many devices from destruction consists of strict adherence to the maximum values of voltage and current as specified for the device in question, and also in adoption of a common ground potential for all connected equipment. All testing should be made with a 5V power supply with a current limit capability.

Set the current limit of the supply to 65mA and connect a 6.2V zener diode across the

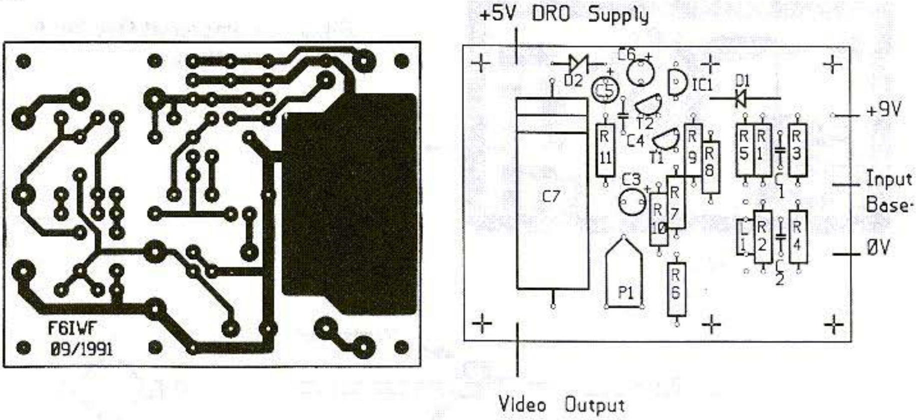

Fig.7: Modulator PCB Layout and Component Overlay (finished size: 56 x 43mm

power supply output. Be careful that the 5V wire does not touch the ground during tests (around the +5V hole of PCB) to avoid producing spikes which could destroy the oscillator transistor.

Note: the oscillator should only be switched on when the resonator is in position.

Hold the cavity horizontally (e.g: in a small vice). Place the resonator between line L1-L2, switch on the power supply, monitor the current with a multimeter and close S1. The current drawn should be between 25 and 50mA. Move your hand over the open cavity, or put the cover on the cavity (the device is a low power type and there is no danger of causing power surges due to hand capacitance, etc.), the current drawn should change as the cover is put on or your hand moved across the cavity, thus showing that the oscillator is running. Measure the frequency with the wavemeter, counter or spectrum analyser and adjust the tuning disc for the required frequency. You can also adjust the position of the tuning disc and observe the effect on a 10 GHz FM TV receiver and tune that way, as long as the receiver is calibrated accurately enough for your purposes.

3.2 Positioning and cutting the resonator

The frequency of the resonator should be adjusted to be lower than the final working frequency by around 100 to 200 MHz (250 MHz being a maximum) because the capacitive effect of the cover when in place will raise the frequency by approximately this amount.

In many cases, with a 10000 MHz resonator the frequency of oscillation will be too low if you want to transmit on the upper part of the 3cm band, therefore it will be necessary to reduce the thickness of the resonator by sanding it down. Using abrasive paper grade 220 or 240, place the resonator on a hard flat surface, make a cross on one side of resonator and sand the unmarked one. Periodically reposition the resonator in the circuit and measure the new frequency. Dependent on the hardness of the resonator's ceramic material the frequency can drift up to 200 MHz over a period of from 5 minutes to 1 hour. When the desired frequency has been achieved by sanding clean the resonator with acetone or similar cleaning agent.

If the resonator frequency is too high, it is possible, in principle, to put a ceramic support underneath the resonator. However, it is more practical to use an epoxy-glass PCB ring, provided that it is not required to lift the resonator by more than 1 to 1.5mm above the substrate, more than this may cause some instability.

Before finally fixing the resonator in position (by a drop of cyanoacrylate glue), it is necessary to test the transmitter fully. Fit the cover on the oscillator and tune the screw to obtain the desired frequency. Connect the power supply to the modulator and connect a 1V peak-to-peak colour video source. Check the picture quality on a TV receiver. If satellite receiver is used as the final receiver you should obtain a video output signal of 1V peak-to-peak across a 75 ohm load with potentiometer P1 at midway, which corresponds to a transmit deviation of around 20 MHz.

Note: when the resonator is moved near the transistor's gate line, the coupling decreases and the deviation increase, the modulation is better but the power output is less. In practice, the best resonator position was found between the lines L1-L2 against the transistor ground pin, slightly towards the drain line but not going over it. At the working frequency the metal tuning disc should be approximately 1mm above the resonator. Once the optimum position has been noted, put a small drop of glue under the dielectric cylinder and fix it in place.

Permanently wire the power supply and modulating signal input connections through the cover and screw it tightly in position. Adjust the tuning screw for the desired frequency and tighten the lock nut. Confirm that the required deviation is obtained when a modulating signal is applied, before sealing the unit in its weatherproof housing.

4.
Housing and Waterproofing

As this microwave source is probably intended to be used outdoors, it is necessary to provide a weatherproof system (Fig.8). It must be either completely weatherproof or permit the permeation of air. You must not make it "almost" waterproof, because water could accumulate in the box due to condensation from the incoming air. I chose the complete weatherproof method

Construct an enclosure from epoxy-glass PCB material. Mount RCA plugs on the bottom, solder quickly so as not damage them, the solder joints should also be weatherproof. Then, solder together sides and bottom to make a box. Solder threaded posts in the corners for the lid, connect 10cm wires to the RCA plugs and ground and waterproof with silicone rubber. Fix the transmitter inside the housing, connect the wires from the RCA plugs to the DC input, modulating signal input

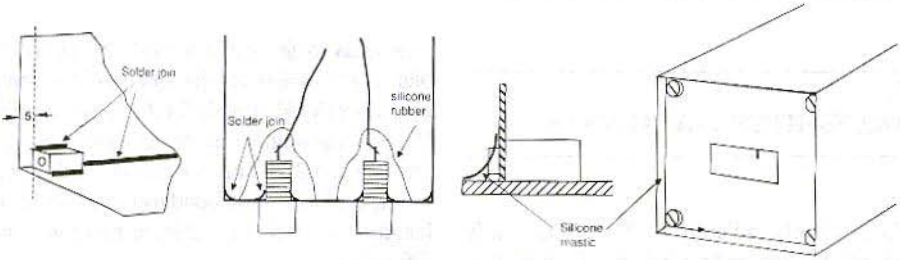

Fig.8: Details of the Waterproof Housing

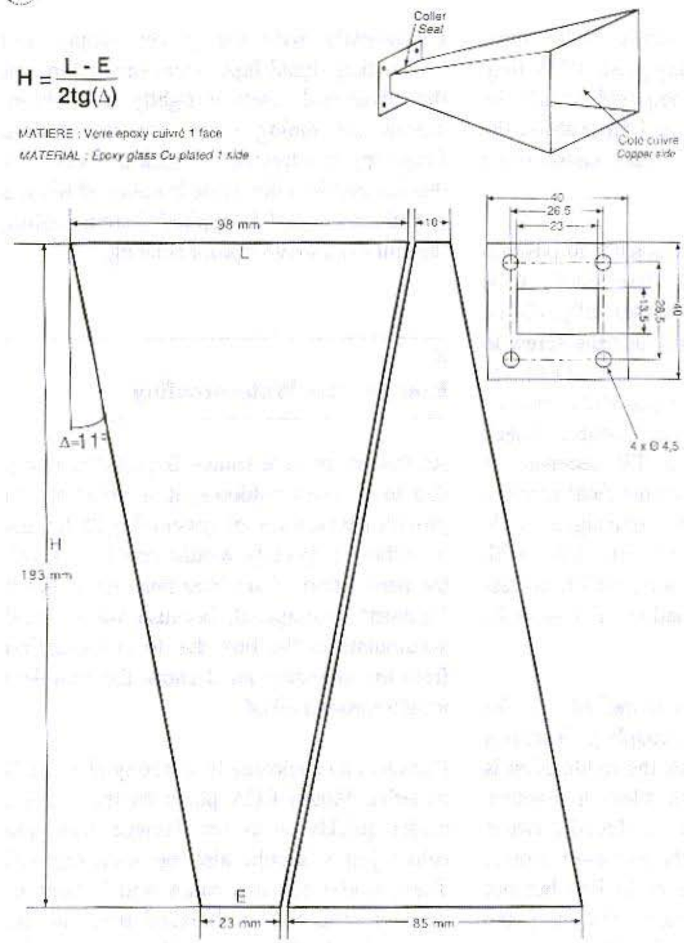

Fig.9: Details of the Horn Antenna

effective radiated power of around 4W from our 40mW input.

Solder together the epoxy plates (copper side inside feed). Fit and put the flange on the feed (copper flange side to the cavity) and roughen surfaces to be sealed. Seal with a two-part epoxy sealant and wait for it to completely set.

For outdoor use it will be necessary to place a 0.05 to 0.15mm thick PTFE film between the feed and source, held in position by a thin film of silicone sealant. Then fix the feed-horn onto the output flange of the transmitter.

and ground accordingly, coat the cover screws with silicone sealant and fix the cover in position, again with sealant on all the joints.

5. TRANSMITTING ANTENNAS

To efficiently radiate your 30 to 40mW it is advised to construct a 20dB feed-horn such as the model shown in Fig.9, which will give an

6. OPERATION AND TEST RESULTS

The feeds to the unit are made by using 75 ohm coaxial cable for the video and by using coaxial or shielded cable for the power supply. If the transmitter is to be permanently mast-mounted, make all cables and plugs waterproof with a self bonding tape. The cable lengths can reach 20 to 25m or more without difficulties.

For transmitting picture and sound, it will be necessary to use a a separate audio and video mixing stage, which will add the 6 MHz audio subcarrier to the video baseband signal before it is input to the modulating stage.

Many tests were carried out with the prototype transmitter under the following conditions: transmit power 15 dBm; antenna gain 20 dBi; atmospheric loss 0.2dB/Km (normal rain); Bandwidth 27MHz; deviation 17MHz.

Two different receive systems were used and typical results obtained are given below:

6.1 ''New receiver'' version:

A modified satellite converter with a noise figure of less than 2dB, and a 50cm antenna with 70% efficiency. Distance 20Km.

Results: Carrier to noise ratio approximately 22.7dB (margin about 13 dB - note that a C/N of at least 10dB is required to obtain a correct picture) and a Video signal-to-noise ratio of approximately 56dB (professional quality).

6.2 ''Classic receiver'' version:

A traditional Gunn mixing diode system with a noise figure of less than 8dB and a 30cm antenna with 50% efficiency. Distance 15Km.

Results: Still good with a C/N ratio of approximately 14dB (4dB of margin) and a video S/N of approximately 47dB, corresponding to a very good TV picture.

COMPONENTS LIST

MODULATOR

R1, R2 : 75 Ω
R3, R4, R10 : 150 Ω
R5 : 22 Ω
R6 : 390 Ω
R7 : 10 KΩ
R8 : 39 KΩ
R9 : 470 Ω
R11 : 680 Ω

P1 : 100Ω PIHER

C1 : 1nF
C2 : 680 pF
C3 : 22 µF/16V Chimical radial
C4 : 100 nF plastic
C5 : 4,7 µF/25V Chimical radial
C6 : 1 µF/25V Chimical radial
C7 : 470 µF/16V Chimical axial

L1 : 10 µH

D1 : 1N4004
D2 : Zener 6,2 V 0,4 W

T1, T2 : BC238B

IC1 : 78L05

Circuit : 1 side epoxy glass

OSCILLATOR

R1 : 100 Ω CMS
R2 : 51 Ω CMS (not critical)
R3 : 10 Ω CMS

C1 : 1 nF CMS
C2 : 100 nF CMS

D1 : LL4148 (mini-MELF) or 1N4148 with leads cut to 1 mm

T1 : ATF26836 AVANTEK .

DR : $TE_{01\delta}$ mode dielectric resonator 10 to 10,4 GHz (see text), diameter 5.5 to 6 mm. It can be removed from a defective "ECS/ASTRA" satellite converter.

Circuit : 2 sides teflon-glass εr = 2,55 thick 0,79 mm

Pins : silver plated wire Ø 0,8 mm

Transistor ground pins, Antenna : silver plated wire Ø 1,2 mm

Cavity :
- tin-plate 1mm (WR75 output flange)
- tin-plate 0,5 mm (shielded box, cover)
- 1 x screws M3 x 10
- 3 x nuts M3
- 4 x screws M2 x 4
- 4 nuts M2
- 4 closed nuts M4

Detlef Burchard, Dipl.-Ing., Box 14426, Nairobi, Kenya

Absolute Calibration of a Noise Source

Semi-conductor noise sources have become common everywhere for determining the noise levels of receivers. As against the tube diodes used earlier, they have the advantage of a very long life and the disadvantage that their excess noise ratio can not be derived from a natural law. They must be individually calibrated!

To this end, a primary standard is required, which can be, for example, a tube diode noise generator.

Should no standard be available, an absolute calibration can still be carried out, which need not be as accurate as that of industrial products.

The present article gives three methods, which differ as to cost and precision. A receiver, a signal generator and a digital voltmeter are virtually all you need.

1. DEFINITIONS AND PRINCIPLES

According to the Nyquist formula, the noise output available from an ohmic resistance during tuning is:

$$P_r = k * T * B \qquad (1)$$

k = Boltzmann's constant: $1.38.10^{-23}$Ws/K
B = Band width in Hz
T = Absolute temperature in K

At the reference temperature, 290 K (+ 17° C), therefore, it is 4.10^{-21}Ws (or W/Hz) and corresponds to -174 dBm/Hz. The "strength" of noise sources, the excess noise ratio, is a dimensionless factor, which indicates how many times higher the available noise output is than the thermally generated noise output, in accordance with equation (1). The German expression which describes this best, although

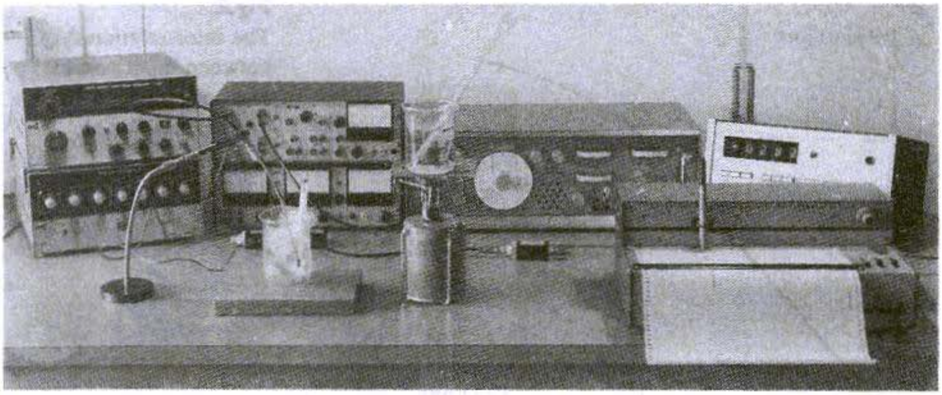

Fig.1: Equipment required for Calibrating a Noise Source:
Rear left to right: signal generator; next bottom, power supply for semiconductor noise source; on top, multi-function unit containing two 30dB broad-band amplifiers which ensure low-noise input and/or decoupled intermediate frequency output before or after the laboratory receiver; a laboratory receiver; finally a digital voltmeter with 10uV resolution.
Front left to right: home made 50 ohm sensor, home made noise generator (partially covered by glass), glass containing melting ice, glass containing boiling water. The chart recorder at the front right is for documentation purposes only.
The home made measuring head can be seen in front of the receiver.

an unfamiliar one, is the "Rauscherhoehungs-faktor" (noise increase factor). It is calculated in dB, so here I shall describe the expression 10.lg ENR as the noise increase dimension and use ENR/dB as the formula. This happens in an analogous way to additional values, which present themselves both as factors and as logarithmic dimensions (Table 1).

Here we are using only outputs for calculation. So you can mentally put the word "output" before all these expressions. With the logarithmic values, that soon becomes apparent anyway from the 10 in front of the logarithm.

A noise source with noise increase factor 35.482 (ENR/dB = 15.5) can be imagined as an ohmic resistance at a temperature 10,000 K higher -sensor (10,000 + 290) - 290. Because of this interaction, industrially manufactured noise sources are predominantly supplied with a noise increase dimension of 15.5dB.

Noise factor F	Noise dimension F/dB = 10.lg F
Change factor Y	Change dimension Y/dB = 10.lg Y
Amplification factor G	Amplification dimension G/dB = 10.lgG
Damping factor a	Damping dimension a/dB = 10.lg a
Reverse damping a_r	Reverse damping dimension a_r/dB = 10.lg a_r

Table 1

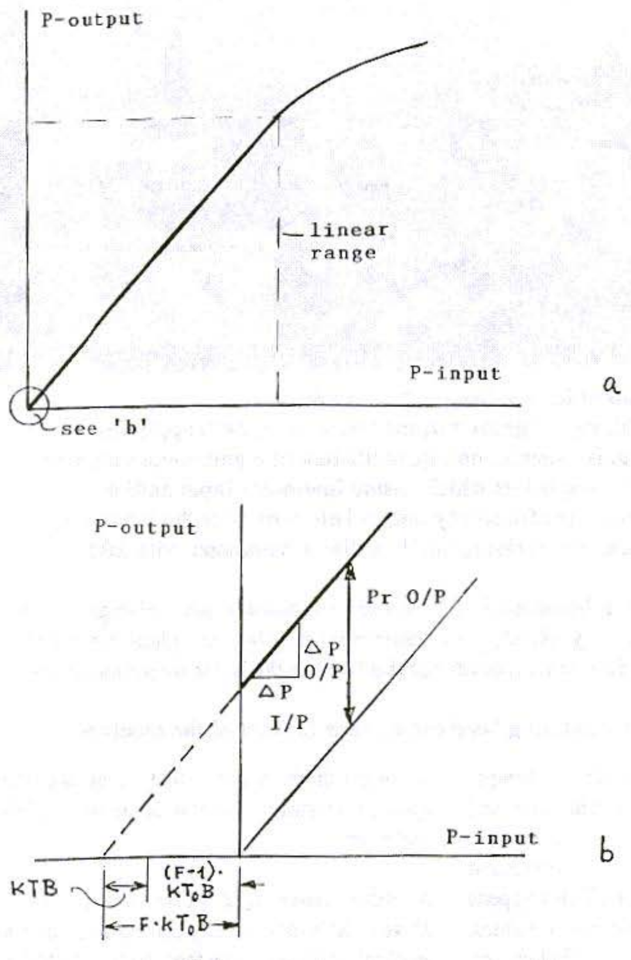

Fig.2:
The inter-relationship between input power and output power for a linear amplifier at:
a: high level
b: low level

In spite of the enormous apparent increase in temperature, the noise output thus generated is still so small that it must be amplified before it can be displayed using the normal output meters at, for example, - 40dBm. If the band width of the amplifier is 1Hz, then we need approximately 120dB amplification, if 1 kHz/ 1 MHz/1 GHz, then 90/60/30 are the figures required. Not until 1 THz would there be sufficient output to show up on the output meter referred to earlier. Unfortunately there are no broad-band noise sources or output meters of this nature. Moreover, for reasons of quantum mechanics, formula (1) applies accurately enough only up to approximately 100 GHz. On the other hand, we are not normally interested in the average noise increase dimension over a large frequency range, but rather within quite specific narrow frequency bands. A flat-line pattern can be obtained over a large frequency range. This is advantageous, but not absolutely essential.

Amplifiers have internal noise sources of the same order of magnitude as the noise sources to be calibrated. So if amplifiers always have to be used to calibrate a noise source, then we must initially busy ourselves with the amplifier noise levels. And here we are including as amplifiers those with single frequency conversion or multi-frequency conversion, which have a defined band width in the frequency plane and which also have defined amplification, i.e: a linear relationship between the output power and the input power.

This relationship is shown in Fig.2a. The curve does not show one important detail at the origin. If we draw the zero point area on a larger scale (Fig.2b), it then becomes clear that the curve does not meet the zero point, but meets the ordinate at a positive value. The noise output power, PROutput is the noise output given out by the source resistance at the input and amplified in the amplifier, plus the noise output generated in the amplifier itself. Without any further consideration of where the noise source within the amplifier is concealed, we can assign its effect to the input, i.e. we can act as if this noise output were also subjected to the complete amplification. The noise factor of the amplifier is a dimensionless number, which gives the factor by which the noise of the source resistance is increased in accordance with equation (1). But since it can be measured only at the output, the determination equation

$$F = \frac{P_{R\,Ausgang}}{P_{R\,Quelle} \cdot B \cdot G} \qquad (2)$$

applies, or else

$$F/dB = P_{R\,Ausg}/dBm + 174\ dBm - 10 \cdot \lg B/Hz - G/dB \qquad (2a)$$

Only in special cases (low-frequency amplifiers) can the source resistance be made zero, so that the amplifier noise can be measured on its own. In the high-frequency range, all active and passive components alter their properties if the system resistance (usually 50 ohms) is deviated from.

Should the noise output of a noise source now be fed to the amplifier input, then the output power increases by the change factor, Y. The relationship existing between the ENR, F and Y is as follows:

$$ENR = F \cdot (Y - 1) \quad \text{or} \qquad (3)$$

$$ENR/dB = F/dB + 10 \cdot \lg (Y - 1) \qquad (3a)$$

This formula is normally used to determine F, with the help of a noise source. Naturally, it can also be used to determine the ENR if an amplifier with a known noise factor is used. If the ENR is known, then conclusions can be drawn about the amplification from the measured increase in the output power and vice versa. It is very frequently true, as indicated in Fig.2b, that the amplification is the quotient obtained from the output power increase and the input power increase. In a completely linear area, we can measure an input power increase of any size as a corresponding output power increase. Thus we do not need particularly low-noise amplifiers to calibrate a noise source. We need only a high-resolution power meter.

A power meter of this type operates through a diode measuring head and a digital display. Anyone who has existing apparatus from HP, Marconi or R & S is already over-equipped. Because in fact we shall predominantly be measuring power ratios, absolute calibration is not required. Vieland-type equipment (5, 7) is also very suitable. A diode measuring head in front of a high- resolution digital voltmeter (10uV or better) is suitable, as is one of the many DVM models with 3.3 places and a minimum measuring range of 200.0mV, to which a chopper amplifier is connected in series, in accordance with Fig.3. The diagram also shows how the zero connections must be effected so that noise loops in coaxial cables and thermal stresses do not have any effect on the rectifier.

The diode measuring head operates in accordance with a natural law which we can rely on implicitly at rectified voltages of up to 10mV. As Burchard (1) has demonstrated, the rectified voltage is as follows:

$$U_{Richt} = \frac{1}{2} \frac{\hat{U}^2}{U_T}$$

$$\hat{U} < 2 \cdot U_T$$

$$U_T \approx 40 \text{ mV (AA 119)} \qquad (4)$$

A peak factor of 8 is sufficient for the correct evaluation of noise with Rayleigh distribution (excess probability for 1/2,000 of time). This measuring head then has an input power range of between - 54 and - 21 dBm (rectified voltage of 5uV to 10mV). A doubled reading indicates a doubling of the input power. An increase by a small amount - and here it is irrelevant whether the previous value was low or high - indicates that the input power has increased by an equally small amount. The determination of a change factor, Y, becomes particularly easy. It is simply the quotient of the two figures indicated.

2. NOISE GENERATORS

Home-made models can be designed like those of Ulbricht (4), Fleckner (2) or Rohde (3). What is common to all of them is that current is sent through a semi-conductor junction with zener or avalanche properties. If the current can be switched on and off, then we have a cycled noise source, the temperature of which can be converted from the reference temperature to a much higher one. Unfortunately, the differential diode resistance changes considerably at the same time. A good match with the system resistance can be obtained only by using damping elements. The desired noise increase factor can be set by the selection of the damping factor. All the noise sources referred to above initially give ENR at 35dB, and can therefore be reduced to the desired value by means of 20dB damping. This simultaneously increases the structural return loss in the desired fashion to approximately 40dB.

There is an optimal current for each example of a noise- generating PN junction. The semi-conductor noise source is not adjustable as is the case for a tube diode. It more closely

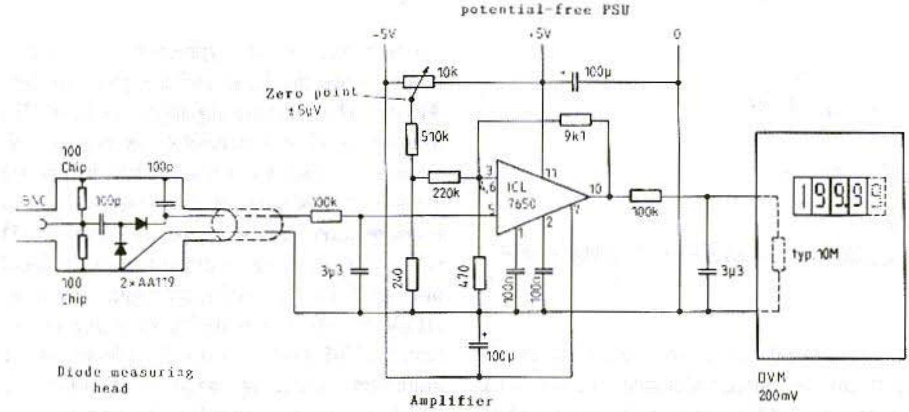

Fig.3: Circuit for a high-resolution home made Power Indicator

resembles a noise-generating gas discharge, and there is a model which accounts for the noise using an inter-crystalline plasma in the semi-conductor. For this reason, the optimal current must first be found for any home-made noise source.

A variable-frequency receiver can be used to establish whether the noise is white, and therefore independent of frequency. Look for the current level at which this requirement is best met. In principle, this can be done using the laboratory receiver in Fig.1, although it is a laborious task.

Because documentation is easier, a spectrum analyser was used behind the 30 dB amplifier, and thus we obtained Fig.4. With this semi-conductor example (BF324A), a current of 200uA was revealed as correct (Fig.4b). The value is not critical, +/- 20% can change the picture.

However, if the current is tripled, or reduced to a quarter (Fig's.4a and 4c), there is a larger spectral power density, although it can scarcely be called white. The reduction above 600 MHz is because of the wide-band amplifier, which has an NE5205 in the input

This analyser reading should not be over-valued, because the errors can be considerable. The frequency level of the preamplifier (without which most analysers will in general not give a picture which can be evaluated) is a contributing factor, as are those of the calibration divider and the first mixer, as well as the conversion error of the logarithmic converter. You can't expect much better than 1 to 2dB!

The analyser or receiver used, however, makes possible an initial estimate of the noise increase dimension! Here we are using method 1.

3. ABSOLUTE CALIBRATION

3.1 The noise factor method

If you have a receiver with a known noise dimension and a determined change factor, Y, then you can also calculate ENR using equation (3). The example below, together with all following examples, refers to the structure shown in Fig.1 at 150 MHz.

From Fig.4b, we read off Y/dB = 10. The amplifier has a typical noise dimension of 6.5 dB. Y - 1 is 9, so that finally we obtain ENR/dB = 16.

The procedure is permissible if the noise dimension of the amplifier is determined by a law of nature. This is largely the case with the NE5205. Its noise predominantly comes about in internal feedback resistances. This also applies to many other gain-blocks.

If the change factor, Y, is determined using a power indicator, then this can be done with great accuracy. The measurement error here depends almost entirely on the accuracy with which the noise dimension is known.

3.2 The substitution method

The noise source to be calibrated generates an output increase at the amplifier output which is given by the input power, PR, as per equation (1), multiplied by ENR and the amplification factor. PR contains the effective noise band width of the amplifier, which in general deviates from the -3 dB band width. Using the substitution method, another, known signal source is now connected to the input after the noise source to be calibrated, and the output power increase caused by this is measured.

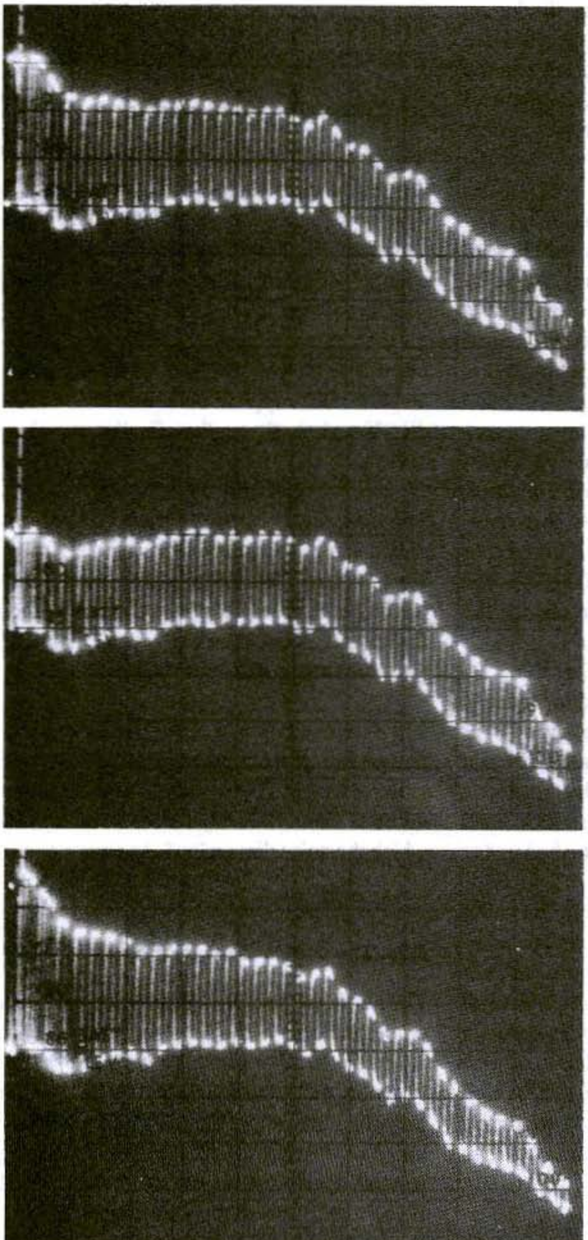

Fig.4:
Spectral power density of a semiconductor noise generator at various operating currents:
a: 650uA
b: 200u;
c: 50uA
X: 0-1 GHz (100 MHz/div)
Y: -135...-95dBm (5dB/div)
Bandwidth: 200 kHz
Video Filter: 100 Hz
Sweep time: 3 seconds
Switching frequency of noise source: 15 Hz

If the second source is likewise a noise generator, then we do not need to know the noise band width. From the two change factors and the known noise increase factor of the comparison source, we can immediately calculate:

$$ENR = \frac{Y_1}{Y_2} \cdot ENR_2 \quad \text{oder} \tag{5}$$

$$ENR/dB = 10 \cdot \lg \frac{Y_1}{Y_2} + ENR_2/dB \tag{5a}$$

It is possible to simplify the measurement if the comparison source has adjustable power (tube noise generator). If we actually make Y2 equal to Y1, then we have made ENR = ENR2 and can read the value off directly from the comparison generator.

If the comparison generator is a signal generator with a sine signal, then it is tuned to the maximum value of the response curve of the amplifier. ENR can then be calculated as:

$$ENR = \frac{Y_1}{Y_2} \cdot \frac{P_{Gen}}{k \cdot T_0 \cdot B_{eff}} \quad \text{oder} \tag{6}$$

$$ENR/dB = 10 \cdot \lg \frac{Y_1}{Y_2} + P_{Gen/dBm} + 174\ dBm - 10 \lg B_{eff}/Hz \tag{6a}$$

In this equation, B_{eff} is initially unknown, but can immediately be detected using the equipment available. The effective noise band width is defined by:

$$B_{eff} = \frac{1}{G_{max}} \int_0^\infty G(f)\, df \tag{7}$$

In practise, continuous integration is replaced by step-by-step formation of totals,

$$B_{eff} = \frac{1}{G_{max}} \cdot \sum_0^\infty G_n \cdot \Delta f, \tag{7a}$$

where the stages have to be measured sufficiently precisely. The integration limits, 0 and infinity, indicate that all secondary reception points are included. It can thus be assumed that they are being damped by 30 dB or more, otherwise the noise power received there would be making a noticeable contribution.

Fig.5 demonstrates the experimental reception of the noise band width. The signal generator is changed to the frequency step by step, beginning with frequencies at which the basic noises have not yet been noticeably increased, and ending with the same criterion. The sum of all increases, G_n, over the background noise, divided by the highest value, G_{max}, and multiplied by a frequency stage, gives the noise band width.

The filter of the laboratory receiver measured here is a Bessel filter with a nominal band width of 200 kHz. The noise band width was measured at 258 kHz. We paid attention to the fact that measurement could be carried out using a very low input power -102dBm (approximately 11dB above the background noise) and was nevertheless most accurate.

Fig.6 is intended to make substitution using the signal generator clearer still. First, a stepped curve was plotted, with the generator power set at values from -107 to -103dBm, and then the noise generator to be calibrated was connected. Now, by interpolation between the steps, the noise source can be determined as equivalent to -104.8dBm or calculated by means of the change factor, Y (on the basis of the -104dBm step, we obtain -104.88dBm, but on the basis of the -105dBm step it is -104.83dBm, which points to 1dB stages which are not quite correct). Using equation (6a), we obtain ENR/dB = 15.

Measurement errors are predominantly due to possible inaccuracies in the output power of the signal generator. For the model used here, the error can amount to +/-2dB. It is made up of the error in the volume control plus that of

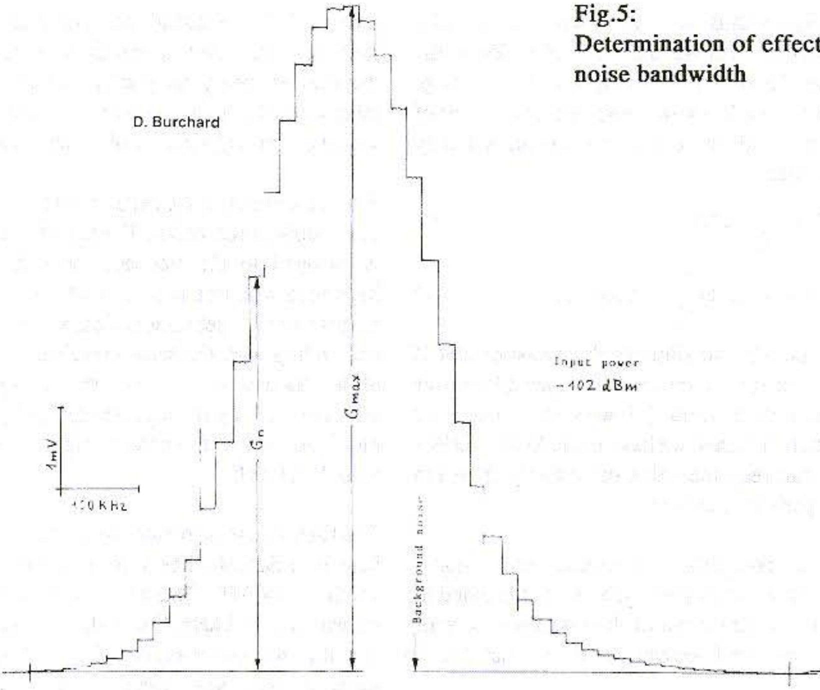

Fig.5: Determination of effective noise bandwidth

the calibration divider. If it is desired to obtain better accuracy, then an external calibration divider of greater accuracy can help, with simultaneous measurement of the input power supplied to it (feed-through measuring head).

3.3 The temperature method

Until now, we had assumed that the noise resistance was at the reference temperature, 290K. That is certainly not always true, because the apparatus also warms up. However, the error caused by this is normally small in comparison to all the others. We now elevate this effect into a principle! The line entered on the abscissa in Fig.2, to the left of the zero point, F . k . T_0 . B, is made up of the thermal noise levels from the source resistance k . T . B and the amplifier noise. We can change the first section if we expose the source resistance to different temperatures.

Such warm-cold standards are commercially available. We are assisted by a metal film resistor, which is exposed to the temperature of melting ice (273K) or boiling water (approximately 373K, depending on the air pressure). Its noise power then changes to approximately 0.34k . T0.

The power indicator, as per Fig.3, can resolve this small change without problems!

Next I soldered on a sensor, as sketched in Fig.7. It must be water-tight, so that the resistances remain dry, and be able to withstand pressure changes which arise internally at the different temperatures. Multiple dipping in polyurethane lacquer is sufficient. Pressure changes obviously balance out due to the short piece of coaxial cable and the ventilation in the plug. A structural return loss measurement using a rho-bridge (Fig.8) can determine whether it remains tight. Here, a is the

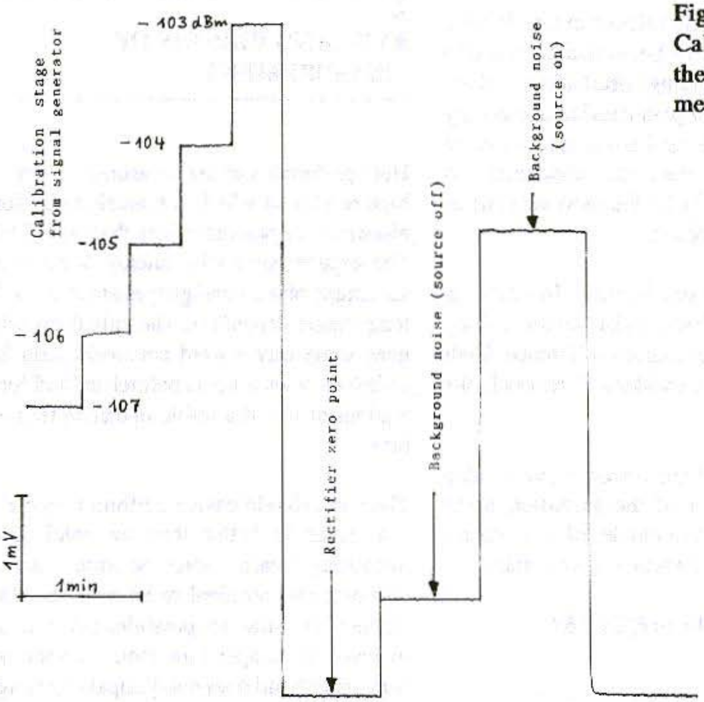

Fig.6: Calibrations using the substitution method

reference level for a_r = 1(a_r/dB = 0), b is the a_r/dB curve for a good sensor and c indicates that a small amount of water has penetrated. Should the resistances be completely under water, then a_r is already measured at under 200 MHz at 10dB, and the sensor has become unusable.

The actual measurement is carried out as per Fig.9. The amplification selected for the rig is as high as possible, and the background noise should almost reach maximum recording level on the power indicator. The difference between the readings from the cold and the warm sensor is then determined. In Fig.9, it reflects a temperature difference of 95K (in Nairobi, because of the height, water boils at 95 degrees C !), i.e: 0.328k . T0. This completes the calibration of the display.

Then the noise generator to be calibrated is connected up. ENR/dB = 15.5 is too high here, and a defined damping element must be inserted in order to get close to the calibration power change. Here we used such an element, with 19.8dB available, measured accurately. When the noise source is switched on, together with the damping, the reading goes high, to 0.398 k . T0, with a change factor of Y = 0.398. The noise increase dimension before damping, then, is:

$$ENR/dB = 10 \cdot \lg Y + a/dB, \qquad (8)$$

which here is 15.8dB.

The measurement error can be kept low if the temperature difference is determined as accurately as possible (use a thermometer) and the statistical measurement variations are kept small. Because of the high amplification, the final positions of the display can change at random, and a further increase in the time constants for the integration elements in Fig.3

may be indicated. The values can then be read off with more security, but measurements take longer. The remaining oscillation (here +/-10uV) can be comprehended as uncertainty of measurement. Should the measured value itself be 160uV, then the uncertainty is +/-0.27dB. This is by far the most accurate of the procedures proposed.

Improvements can still be made by using an amplifier with a lower noise factor and by having a wider temperature difference. Both are intended to obtain wider differences in the reading.

And we can now obtain a more precise value for the noise factor of the amplifier, using Fig.9. From the magnitude of the values recorded or the numbers noted, we obtain:

$$F = 4.6 \text{ or } F/dB = 6.6$$

4. AVOIDING ERRORS OF MEASUREMENT

Here performances are measured with a very high resolution which is scarcely to be found elsewhere in practise (finer than +/-0.01dB). The experimenter will quickly discover that all sample objects and gauges are more or less temperature dependent. The only thing which goes some way toward countering this is to switch on several hours beforehand and let the equipment run at a stable operating temperature.

The room should have a uniform temperature - a cellar is better than an attic! Diode measuring heads, noise sources, damping elements and terminal resistances should be touched as little as possible, since a 10K increase in temperature from contact with someone's hand does not dissipate itself again completely until half an hour later!

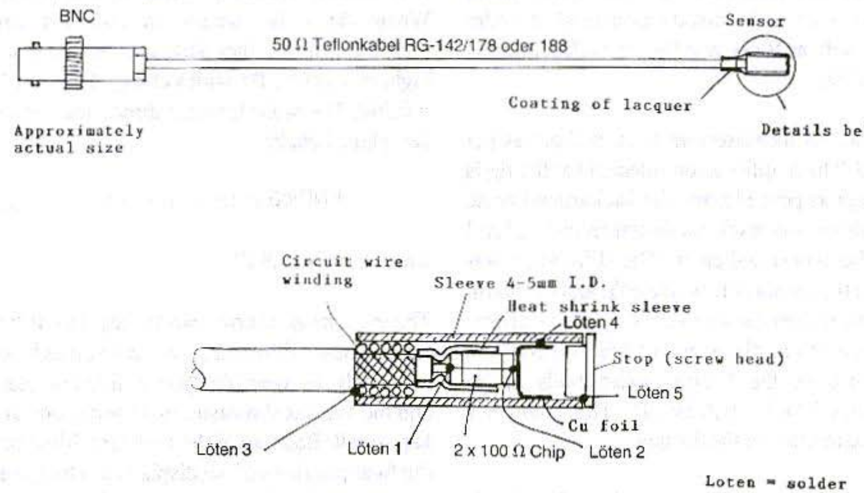

Fig.7: 50 ohm Sensor for temperature method

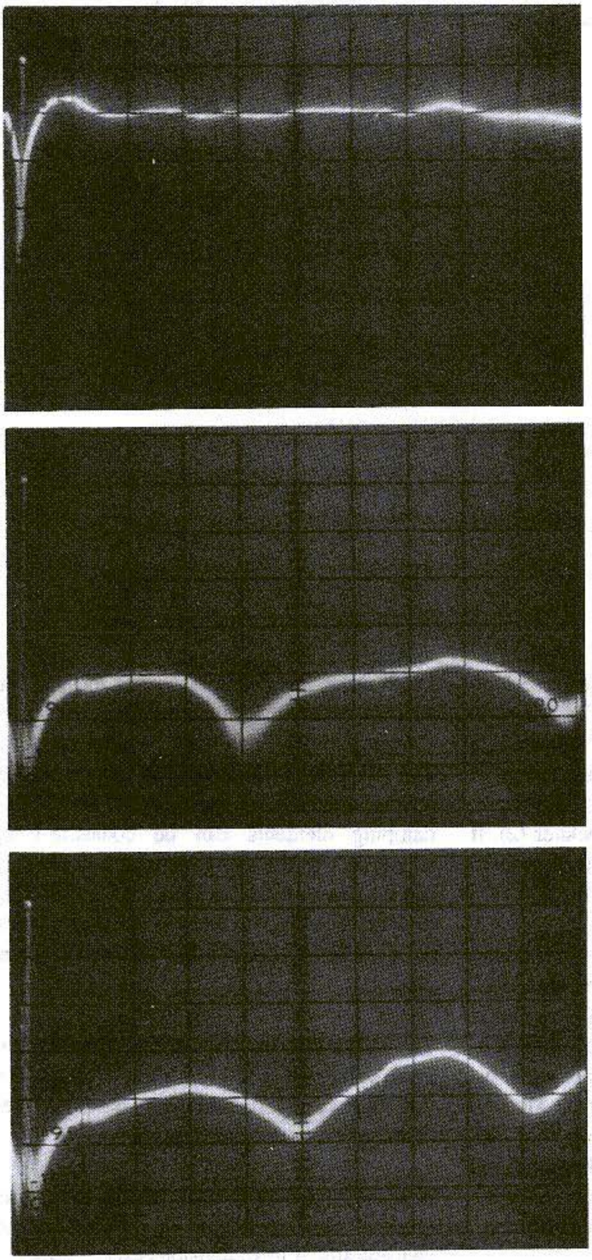

Fig.8:
Structural return loss of a 50 ohm Sensor measured using a rho-bridge.

a: ref. line for a_r = 0dB
b: measurement curve for good sensor
c: after slight water penetration
X: 0...500 MHz (50 MHz/div)
Y: 10dB/div (ref. line see 'a')

Bandwidth: 200 kHz
Video filter: 10 kHz
Sweep period: 1 second

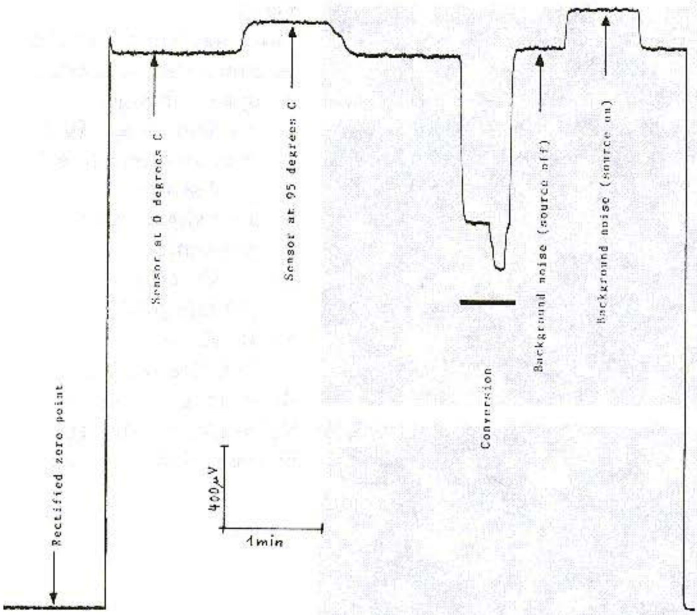

Fig.9: Calibration using the temperature method

All sources and terminals should have high structural return loss values. The absolute bottom limit is 20dB. Here 1% of the power is already being reflected, and an error of measurement of the same size can arise. Figures can be read off from Fleckner (2). If you have a minimum of a_r = 30 dB, then there are no problems.

RG cables are good enough, but their damping is not reliable. A section 0.5M long with BNC connections has about 0.15dB of damping at 150 MHz. Make sure that 75 ohm pin-and-socket connectors are not mounted inadvertently. Longer cables must be allowed for in calculations. Their damping, and also that of damping elements, can be measured with a very high degree of accuracy using the signal generator and the power indicator at the desired frequency.

Suitable damping elements can be constructed as per Vieland (6) itself. Here I propose different dimensions, which are aimed at maximising the structural return loss, a_r. At specific resistance values in the E24 range, shown in Fig.10, this happens automatically. The damping dimension is distorted, of course, which is no disadvantage here. Such damping elements can be connected up subsequent to the signal generator if you are not satisfied with the accuracy of the internal divider, or in order to weaken the noise source to a defined extent for the temperature method.

The difficulties increase at high frequencies. From values above 200 MHz, up to 500 MHz, you must very definitely apply the principles of assembly, as described by Vieland (6, 7).

It is very generally true that a structural element can no longer be thought of as concentrated if its dimensions exceed lambda/100. Pin-and-socket connections and cables will no longer be completely tight, which can be demonstrated by bringing them close to each other.

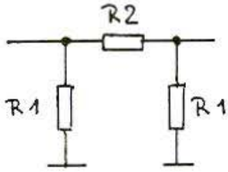

R1/Ω	68	75	120	180	200
R2/Ω	160	120	51	30	27
a/dB	16,33	13,98	7,71	4,96	4,44

$a_r = \infty$ für

$$\frac{R1^2 \cdot R2}{2R1 + R2} = Z_0^2 = (50\ \Omega)^2$$

Fig.10: Damping factors for various values of resistors in the PI network shown above

Sensitivity to manual contact (apart from heating influence) can be triggered by such leaks, but also by outside transmitters, conversion oscillators, digital gauges and standing waves (reflected power). In any case, it must be tuned out before any calibration whatever is undertaken.

Assistance can be obtained from improved screening, extremely short cables, and if necessary altering the measurement frequency or the conversion frequency.

5. SUMMARY

Three methods are proposed which make it possible to calibrate a noise source even in a "cellar laboratory".

The first is suitable for rapid at-a-glance calibration, the second is the standard method (if a sufficiently accurate signal source is available), and the third is based on physical principles and is independent of other standards. If the procedure is carefully carried out, high accuracy is obtained.

6. LITERATURE

(1) D.Burchard (1991): Principles of Rectification of low AC Voltages using Semi-Conductor Diodes.
VHF Communications 3/91, pp. 168 - 174

(2) H.Fleckner (1984): A Noise Generator with defined Noise Output for Applications into the Microwave Range.
VHF Communications 3/84, pp. 146 - 160

(3) N.Rohde (1990): Spectrum Analysis for Electronics Engineers.
Elektronik, 4/90, pp. 90 - 99, Franzis-Verlag, Munich

(4) M.Ulbricht (1981): A Noise Generator for VHF and UHF.
VHF Communications 1/81, pp. 38 - 43

(5) C.Vieland (1983): Sensitive Thermal Power Meter.
VHF Communications 4/83, pp. 225 - 231

(6) C.Vieland (1984): Compact Damping Elements in BNC.
VHF Communications 4/84, pp. 207 - 212

(7) C.Vieland (1987): Diode Detectors in 50-Ohms Wide Band Engineering.
VHF Communications 4/87, pp. 223 - 237

Matjaz Vidmar YT3MV

A very low-noise Aerial Amplifier for the L-Band

A few years ago, the micro-wave elements required for constructing low-noise preamplifiers - especially GaAsFETs - were still very expensive. Any radio amateur interested searched for the active structural elements more on the basis of price and availability than on that of the technical data, and development included, above all, intensive calculation work for the micro-strip circuit. Unfortunately, only a very few papers were ever published on experimental work on the real amplifier circuit, and even fewer involving anything other than micro-strip techniques.

Happily, the prices of GaAsFETs have steadily fallen, and they have steadily become more and more available since these components have begun to be used in mass production - for satellite television receivers. So nowadays amateurs can obtain these components for practically nothing, by stripping down obsolete or faulty satellite television converters. And lastly, amateurs have also learned how to treat GaAsFETs.

Most GaAsFETs were developed to operate in satellite television converters at 11 GHz. In this frequency range, micro-strip circuits are practically all there is on offer in order to create repeatable circuits which are good value, with components of manageable size.

A limitation weighing heavily on the design of micro-strip circuits on a soft substrate with a dielectric constant of between 2 and 3 (PTFE/Teflon) is that the characteristic impedance of the strip circuits can not deviate very far from 50 ohms.

For this reason, all GaAsFETs are manufactured to operate in a 50 ohm environment in the frequency range between 10 and 15 GHz (this also includes the parasitic reactive impedances of chips and housings).

At lower frequencies, these components must be operated with markedly higher impedances - at least, if you want to make use of the improved noise and amplification values.

But these high impedances can be matched only with difficulty in conventional micro-strip engineering. You quickly arrive at very narrow lines, so that, with high impedance/transformation ratios, significant losses can easily arise. In addition, GaAsFET amplifiers can display stability problems at low frequencies. And, finally, the problem of possible over-excitation, through very strong out-of-band signals, must be taken into account.

In this article, a reliable GaAsFET low noise amplifier for the L-band (1000 to 1700 MHz) is described. On the one hand, two stages provide sufficient amplification to make the noise contribution of the subsequent stages (cable, receiver) negligibly small, and on the other hand there is not yet so much amplification that over-excitation problems arise.

Although this aerial amplifier was designed mainly for a GPS satellite navigation receiver (1575.42 MHz), it also gives excellent results at 1.7 GHz (weather satellite reception) and it can also be used just as easily in the 23cm amateur radio band.

1. DESIGN AND CIRCUIT

For an L-band low noise amplifier, the state of the art allows for the use of two types of semi-conductor: GaAsFETs and silicon bipolar transistors. The former offer noise factors below 1dB and at least 15dB amplification, but also bring the risk of stability problems at these low frequencies. The latter, on the other hand, offer stable operation with noise factors above 2dB and amplification values of up to 10dB.

Conventional L-band low noise amplifier circuits operate with a GaAsFET in the first stage, in order to obtain a noise factor as low as possible, and an Si bipolar transistor (or an Si MMIC) in the second stage, in order to guarantee stability. The noise factor of such a circuit is worsened, first by the noise contribution from the second stage and secondly by the micro- strip power losses (especially from the input transformation). In addition, the amplification of an Si bipolar transistor rises from about 10dB at 1 GHz to 40dB and more below 30 MHz, so that the amplifier can easily become over-excited through strong out-of-band signals.

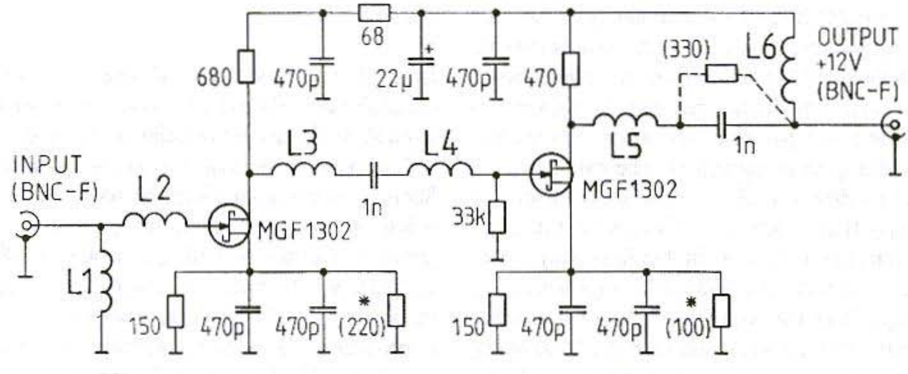

Fig.1: A two-stage GaAsFET Aerial Amplifier for the L-Band

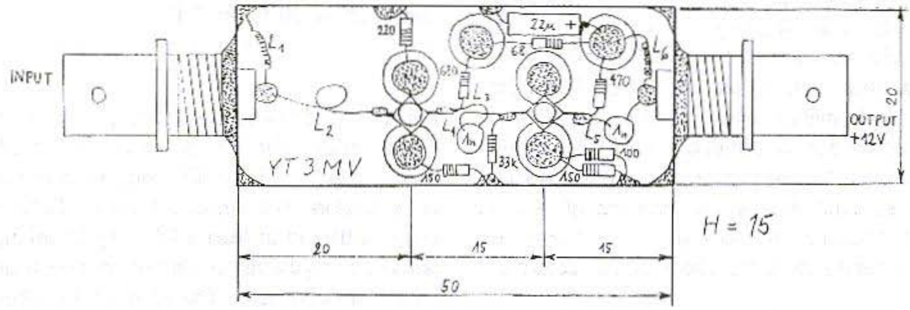

Fig.2: The low-loss structure with air as the dielectric makes an extremely low noise factor possible

For these reasons, the following three design requirements were laid down for the L-band low noise amplifier proposed here:

- Use GaAsFETs in both stages. This provides sufficient amplification to make the noise contribution of the third stage negligible.

- Find a construction method which offers extremely low matching losses (lower than with micro-strips).

- Find a circuit configuration which allows for stable operation under all combinations of surges and loads.

In order to find solutions to satisfy the last two requirements, you should first look at the data on GaAsFETs in the frequency range between 1 and 2 GHz. In this frequency range, you can assume the parasitic reactances of chips and housings to be capacitive. The gate length of all modern GaAsFETs is so short (0.5um. or less) that it has no influence on the high-frequency properties in this frequency range. Gate impedances and drain impedances are high. The real component of an equivalent parallel circle lies in the vicinity of 500 ohms, and the imaginary component is always capacitive in this frequency range.

It follows from this that matching to a 50 ohm system can easily be carried out using series inductances. No additional components, or very few, are required for this. Since a low-noise amplifier represents an extremely low-powered circuit, these inductances can easily be created as concentrated components in the frequency range between 1 and 2 GHz. In practical terms, these small inductances are simply small self- supporting coils with 1 to 3 windings and with an internal diameter of 3mm. If you make them from silver-plated copper wire, the losses of the resulting matching circuit are lower (by an order of magnitude of between 1 and 2!) than those for an equivalent micro-strip circuit. This makes the decisive reduction in the noise factor possible!

In addition to the selection of the components - GaAsFETs and concentric coils - you must think about the assembly technique to be used and the parasitic reactances connected with it. Should you construct a high-resistance circuit using micro-strip technology, then the parasitic reactances will be mainly earth capacitances. In order to reduce them, you should try to bring the characteristic wave impedance of the assembly technique selected into line with the circuit impedances. An assembly technique which is suitable for this

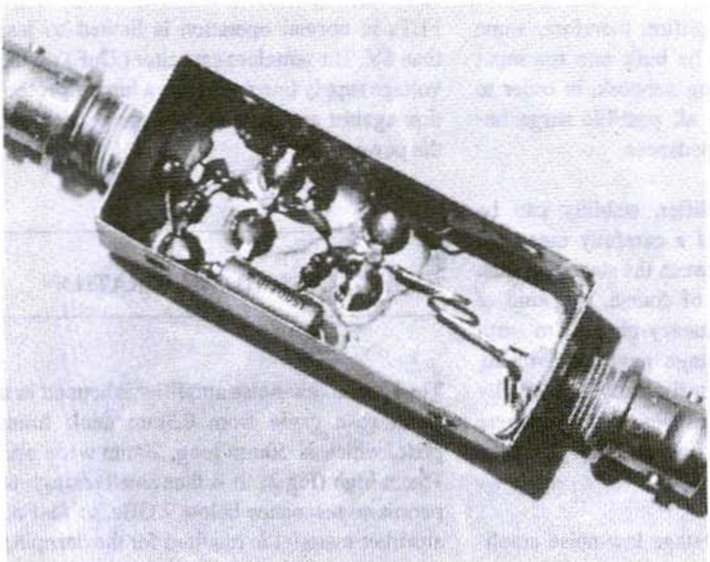

Fig.3: Any radio amateur with some experience in constructing kits can master this layout.

is "round conductor over an even earth surface with air dielectric". In manageable diameter ratios, this layout has a characteristic wave impedance of between 150 and 200 ohms. In practical terms, the components are arranged over a metallic earth surface, and the dielectric is simply air.

Since the parasitic reactances are predominantly capacitances, a GaAsFET amplifier stage will oscillate in the L-band or at lower frequencies only if the input and output are closed off simultaneously with inductive loads which have sufficiently high quality characteristics.

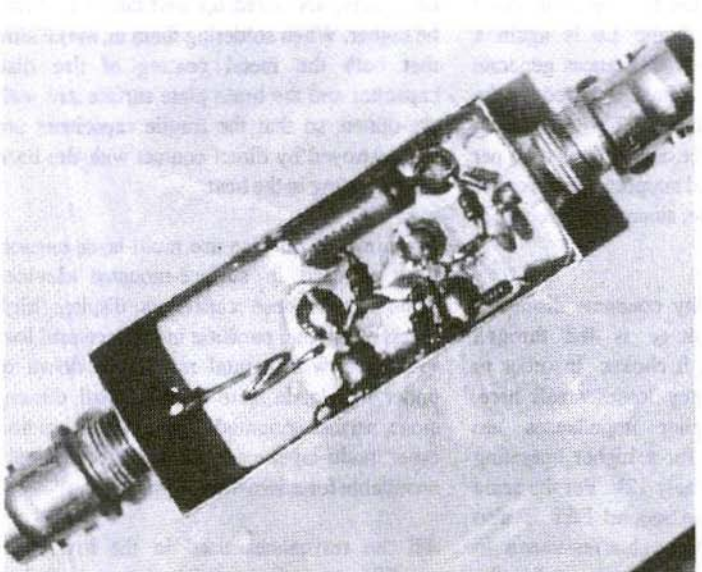

Fig.4: The other perspective brings out further details

In a single-stage amplifier, therefore, some damping (loss) must be built into the input and/or output matching network, in order to guarantee stability at all possible surge impedances and load impedances.

In a two-stage amplifier, stability can be achieved by means of a carefully measured matching network between the stages. In such a matching network, of course, any kind of inductance (high-frequency choke!) to earth or to the supply voltage must be avoided, since it can display a sufficiently high quality at any frequency whatever -often nowhere near the operating frequency - to make oscillations possible.

The circuit for a two-stage low-noise amplifier for the L-band shown in Fig.1 arose out of all these considerations and experiences.

The input impedance matching is provided by L2, while L1 is merely a lambda/4 high-frequency choke. The matching circuit between the stages is a PI network made from the coils L3 and L4 and the parasitic capacitances of the FETs. Finally, the L5 coil is provided for output matching, while L6 is again a lambda/4 choke. Source resistances generate the negative gate bias voltage required for the GaAsFETs in both stages. The de-coupling capacitors for the source connections (two per FET) act as mechanical support points for the circuit at the same time, since the dielectric is just air.

Because of the stability concerns discussed above, the drain voltage is fed through resistances, not through chokes. In order to keep the high-frequency losses small here, resistances with higher impedances are required, which calls for a higher operating voltage than usual, namely 12V. For the same reason, the gate of the second FET is also connected with earth through a resistance. In any case, the drain-source voltage for the FETs in normal operation is limited to less than 6V. The tantalum capacitor (22uF) on the voltage supply line represents a further protection against any possible voltage peaks from the power supply.

2. ASSEMBLY AND CALIBRATION

The L-band low-noise amplifier is housed in a small case made from 0.3mm thick brass plate, which is 50mm long, 20mm wide and 15mm high (Fig.2). It is thus small enough to permit no resonance below 7 GHz, so that no absorber material is required for the damping of parasitic vibrations at these frequencies. The BNC sockets (UG 1094, without nuts or washers) must be soldered on, as shown in Fig.2.

Next, the six 470pF DC blocking capacitors are soldered into the tin case with sockets. They must be ceramic disc or trapezoidal capacitors, not wired up, and their value can be higher. When soldering them in, make sure that both the metal coating of the disc capacitor and the brass plate surface are well pre-tinned, so that the fragile capacitors are not destroyed by direct contact with the base plate bending in the heat.

Warning: In no case use multi-layer capacitors, as used in surface-mounted devices technology! These capacitors display high levels of internal parasitic inductance and loss resistance, with natural resonances down to under 1 GHz. In spite of their small dimensions, surface-mounted device capacitors and other multi-layer capacitors are completely unsuitable for micro-wave applications!

All the resistances used in the low-noise amplifier are wired miniature types rated at

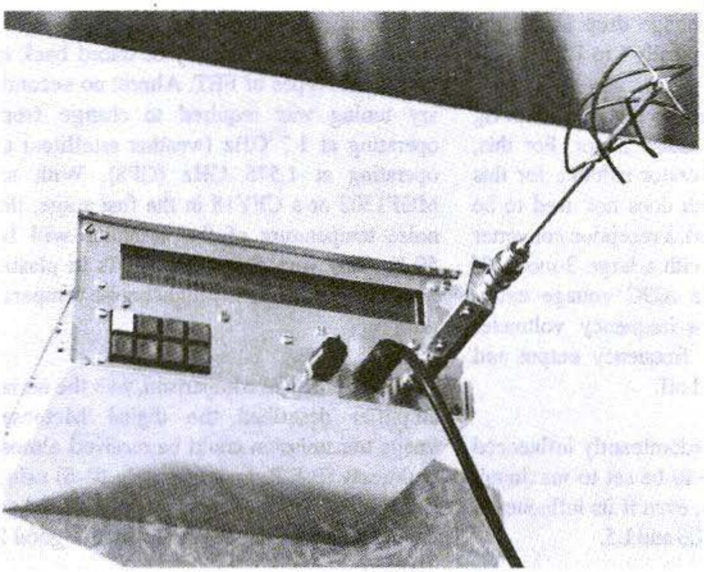

Fig.5: Here the low-noise amplifier described is mounted under the quadrifilar helix aerial on a home made GPS receiver.

1/8W (0204). The source resistances marked with an asterisk in Fig.1 are not soldered in immediately, but are sought out only for the calibration of the amplifier, depending on the ID tolerances of the GaAsFETs used.

The lambda/4 chokes, L1 and L6, are each manufactured from a 6cm long piece of 0.15mm thick enamelled copper wire. The pieces of wire are first broadly tin-plated over about 5mm at each end, and then the enamelled wire is wound around the shaft of a 1mm drill to form a coil. How many windings finally result from this is unimportant. These chokes can be seen tight against the sockets in Fig.3.

L2 is manufactured from a 0.6mm thick piece of silver-plated copper wire. For example, the internal conductor of an RG-214 unit can be used for this. For the frequency range from 1.5 to 1.7 GHz, L2 has a single winding with an internal diameter of 3.5mm (Fig.4).

L3 and L4 simply represent the connection wires of the 1nF disc capacitor between the two transistors (Fig.2) each bent into a half-winding. Similarly, L5 is just a slightly longer connection wire of the output coupling capacitor. The inclination of the loop of L2 and the distance between L3 and L4 are calibrated last, on the basis of optimal data. (Insert Fig's.3 and 4.)

The GaAsFETs are incorporated last. After this operation, you should set your DS working points. In order to avoid any wild oscillations here, the input and output should be terminated with 50 ohms.

The amplifier is now linked to an adjustable voltage source, which to start with should be set to about 7V. The DC between drain and source is measured for both FETs. The thing to do now is to keep both drain-source voltages between 3 and 4V. To this end, you slowly increase the operating voltage and switch the initial source resistances of 150 ohms in parallel again, until the final operating voltage of 12V is reached. Naturally, the parallel resistances should always be soldered on only when the operating voltage is switched off. The final voltage drop across the source resistances is typically 1 to 1.5V.

Now the amplifier must be put into a test rig for amplification and noise factor. For this, you need a noise generator suitable for this frequency range (which does not need to be standard for calibration), a reception converter and an SSB receiver with a large S-meter (if necessary, display the AGC voltage externally), or with a low-frequency voltmeter connected to the low frequency output and with the AGC switched off.

The noise factor is predominantly influenced by L2. L3 and L4 are to be set to maximum amplification, as is L5, even if its influence is much less than that of L3 and L5.

L3 and L4 are normally each up to 10mm long. The distance between the two can be precision-adjusted. L2 can also be precision-adjusted in the same way if you compress or expand the loop somewhat.

If a FET with lower amplification is used in the second stage, such as the MWT11, or an older type from the CFY range, and/or more amplification is desired, then the output network can be modified. The aim is to increase the DC through the second FET. To this end, you remove the 470 ohm resistance and in its place solder in a 330 ohm resistance parallel to the output coupling capacitor. This is shown as a dotted line in Fig.1.

3. RESULTS

Several examples of the preamplifier described were built, using different GaAsFETs made by various manufacturers (some new, some second-hand). The amplifiers gave between 20 and 30dB amplification over a wide frequency range, and the difference in amplification could mainly be traced back to the various types of FET. Almost no secondary tuning was required to change from operating at 1.7 GHz (weather satellites) to operating at 1.575 GHz (GPS). With an MGF1302 or a CFY18 in the first stage, the noise temperature of the amplifier will be 50 K. Only very cheap GaAsFETs in plastic housings gave a slightly higher noise temperature.

To give a practical comparison, with the aerial amplifier described the digital Meteosat image transmission could be received almost faultlessly (B.E.R. approximately 10-6) using a dish aerial with a diameter of only 1.2m And the demodulator losses amounted to a good 2 dB more!

None of the aerial amplifiers constructed showed wild oscillations when connected to an aerial. Wild oscillations could not be detected, even on aerials with high quality, such as a short quadrifilar helix for GPS reception (Fig.5). Of course, this amplifier is not absolutely stable. It can oscillate if the input sees total reflection.

Finally, thanks to the use of FETs, this amplifier is much less sensitive with regard to out-of-band signals than amplifiers with Si bipolar transistors. This can probably be traced back to the uniform reduction in the amplification of signals outside the frequency range in use - in contrast to the sharp gradient of amplification for Si bipolar transistors after the lower frequencies. Practical trials have shown that this amplifier is not even influenced by a 2m or 70cm. transmitter when the aerial amplifier is operating on a radio receiver aerial for GPS (Fig.5) and is only a few metres away from the transmitter aerial. It can be deduced from this that no additional selection is required before or within this low-noise amplifier.

Eugen Berberich DL8ZX

Low-feedback coupling of a Poly-directional Antenna for Contest Operation

1. THE PROBLEM

In contest mode, most antenna formations are used with high gain and thus high sharpness of directivity. The advantage of high gain is countered by the disadvantage of signals from other directions. If you are looking for calling stations, for which purpose a second receiver is perhaps being used, then not much can be heard from other directions.

Assistance in searching for contestants from other directions can be obtained from an additional horizontal poly-directional antenna, or a directional antenna independent of the contest mode.

Two possible solutions are indicated below. One uses a directional coupler, the other a circulator.

2. SOLUTION 1

The coupling of signals from the poly-directional antenna should have as little influence as possible on the existing structure of the installation. Fig.1 shows how a directional coupler is used for feedback-free coupling of a poly-directional antenna. A disadvantage to be pointed out is the coupled damping of the directional coupler, which damps all signals from the additional antenna at 10 dB or more. The damping can be balanced out using a low-noise preamplifier. Directional couplers for this purpose have already been frequently advertised, or can be obtained in the surplus market.

The preamplifier is switched off by a relay during transmission. This relay can be used to switch the poly-directional antenna off for local QRM as well. Only the minute value determined by the sharpness of directivity (20 to 30 dB) is lost.

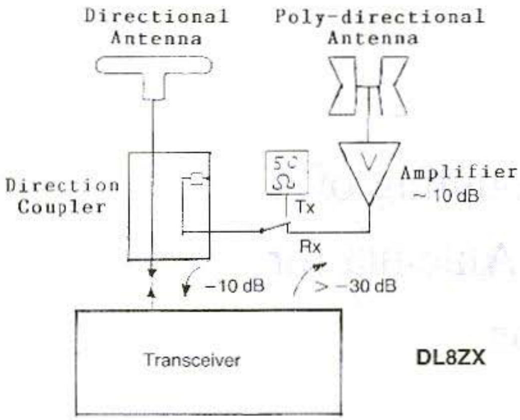

**Fig.1:
Coupling of the signal of an additional Poly-directional Antenna throgh a Directional Coupler**

3. SOLUTION 2

Closer to the ideal solution, but more expensive, is the use of a circulator. This is a ''high-frequency one-ay street'', which is frequently used in commercial antenna couplers, transmitter stages and transmitter combinations. These components used to be common only in the GHz range, but have been found in the VHF range as well for a few years now.

By altering the magnetic flow, a circulator which was constructed for the 2m car telephone range can be trimmed to suit the 2m amateur band. Should a circulator be closed off with a 50 ohm termination at the third connection, it is described as an isolator.

With the help of an isolator, a poly-directional antenna can be coupled through a preamplifier and a directional coupler, without a coaxial relay for the transmission case (Fig.2).

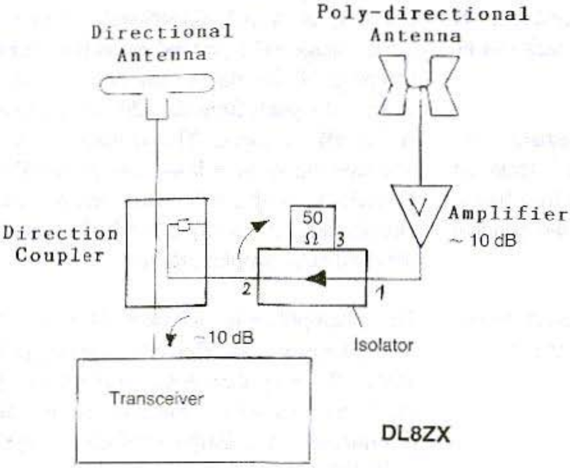

**Fig.2:
An Isolator replaces the Coaxial relay for the Transmission mode shown in Fig.1**

If a poly-directional antenna with horizontal polarisation is coupled in this way, in local QRM the interference signal can simply be reduced through the operating voltage of the preamplifier. The price of such a circulator, of course, is approximately DM 500 (£180) or more, which is an impediment to amateur use.

Another point worth noting with regard to fitting circulators, because of their strong magnetic field, they must not be mounted on a sheet steel chassis or on sheet steel components, since otherwise their high-frequency characteristics can change.

Dr. Volker Grassmann DF5AI

Observation of the 'Multi-Tone Effect'

Temporary distortions in the reception of SSB or CW signals have probably already been observed by almost every VHF radio amateur. Even the author thought this was due to an Aurora band aperture the first time it happened, but then found himself disappointed in this opinion. More detailed investigation shows these happenings to be a very uncommon phenomenon, which can not be explained by simple multi-channel broadcasting and/or velocity modulating effects.

1. SPECTRUM CHARACTERISTICS

In single sideband modulation, the "multi-tone effect" causes a marked distortion in speech, which can be traced back to a widening of the spectrum of the reception signal (7). For carrier-frequency signals, additional spectrum lines arise above and below the actual transmission frequency (1), (2), (6), (7). At 145 MHz, the lateral oscillations display a deviation typically amounting to 30 Hz to 200 Hz (2), (6), (7), and the deviation appears to be greater at higher frequencies. The number of lines varies between one and four (6), but it seems conceivable that more lines could also arise. The individual additional carriers can be observed for between seconds and minutes. During the observation period, the lines are very stable in their frequency (7), and independent in their oscillation behaviour (6), (7). Fig.1 shows the variability of the lateral oscillations on the basis of a measurement at radio beacon DLOPR (144.910 MHz).

The summary of the frequency deviations observed over a time period of approximately one to two hours generally shows areas of accumulation at the onset of lateral oscillations (6), (7). The day before the measurement shown in Fig.1, the summary showed an almost symmetric total spectrum, in which

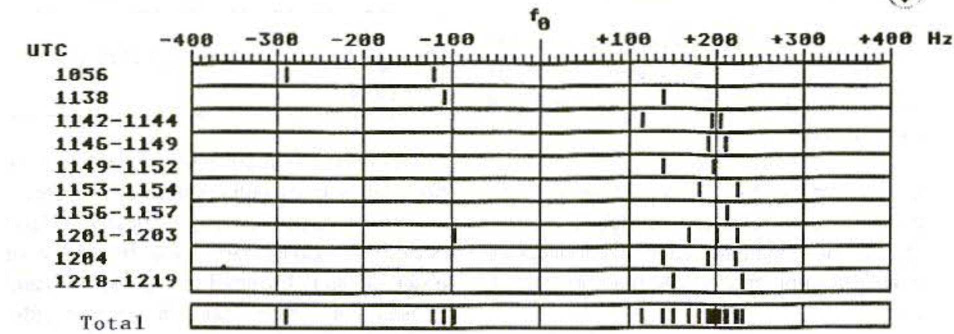

Fig.1: Frequency Deviation due to Additional Spectrum Lines which were observed by the Beacon Transmitter DL0PR. F_0 = 144.910 MHz (05/09/82)

lines were established in multiples of approximately 65 Hz above and below the 145 MHz transmission frequency (6), (7).

Note: Observations from the beacon transmitter DLOPR have been partly confirmed by technical problems with the transmitter at that location, which also led to a serious distortion of the signal. At the time of the observations (1982) DLOPR was permanently beaming an interference-free transmission signal in a Southerly direction.

2. THE INDICATION ERROR OF THE RECEPTION SIGNAL

The direction of incidence of the signal with the wider frequency generally deviates considerably from the true azimuth to the transmitter. The indication error can be greater than 90° (2), (4), (6), (7), Fig.2. Some observations indicate that the direction of incidence of the spectrum lines is slightly

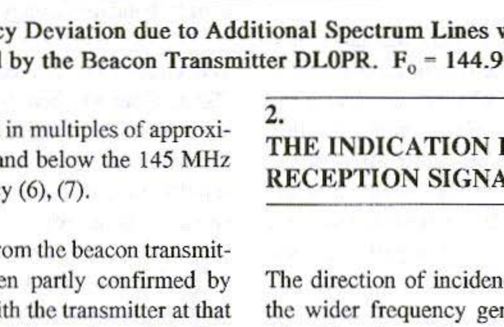

Fig.2: Typical indication error during the observation of the multi-tone effect by Beacon Transmitter DL0PR. The continuously-running transmitter, sited on the North Sea coast, is sending in a southerly direction at an aperture angle of approximately 50°. Drawn in is the direct connection line to the receiver installation in the vicinity of Peine. There the aerial had to be rotated in a south westerly direction to make the effect observable. The aperture angle of the receive aerial is drawn in at approximately 30°. The Great Circle distance is 232km.

different (6) (7). Comparative measurements at various reception sites suggest that the indication error is not a local reception phenomenon (7).

The widening of the spectrum and the indication error are clearly closely connected, for up to now neither an additional modulation or an indication error has been observed on its own.

Research carried out to date has taken into account only the azimuth indication error. Of course, there is one observation where the effect could be observed only at an elevation of less than 44° (8). The orientation of the aerial of the transmitter (approximately 150km away) could be reconstructed, since the station was taking an active part in a moon echo test.

An estimate of the geometric circumstances led to the assumption that the side lobes had participated in the transmission and/or reception aerial when the observation took place. However, it appeared improbable that the phenomenon originated in the troposphere.

The evaluations made it seem more likely that its origin was at a height of approximately 80 to 110km. Unfortunately, it is no longer possible to carry out a detailed evaluation of this observation.

The field strength of the additional spectrum lines is less than the signal level of the transmission signal received on the great circle. If the indication error is interpreted as being due to an extended path of propagation, then the field strengths appear to be greater than those for undisturbed tropospheric propagation over the same distance would be (it will be noticed from Fig.2 that an extended path of propagation leads to trackage of several hundred kilometres).

3. FREQUENCY OF MULTI-TONE EFFECT

Up to now, the multi-tone effect has been observed only by radio amateurs, who report that the phenomenon is practically a daily occurrence. Conceivably, the frequency of observations is favoured by the narrow?band transmission process used in amateur radio (single?band technology and telegraphy).

The effect has been established in the 2m, 70cm, 23cm and 3cm bands. Radio amateurs report that the deviation of the spectrum lines is greater at lower wave frequencies. But simultaneous measurements on different frequency bands are not available as yet. Transmitter stations with relatively high radiated power can be received particularly frequently via the additional signals (5) (7). It is reported that in one case almost all the reception signals one morning coming from a distance of 300 to 500km. were submitted to the effect (4).

4. FIRST INTERPRETATIONS

A few observers explain the phenomenon as a reflection off aircraft (2), (3). Certainly intentional VHF radio links do take place in this way (3), (4), but the constancy of frequency of the spectrum lines established can be adduced as a counter-argument (7). Above all, speeds of approximately 900km/h would have to be assumed to explain the high Doppler shift values, which must naturally be treated as relative motion and not as flying speeds (see (3)). Only aircraft which are landing or taking off rapidly in relation to the observer come into consideration here. Apart from the improbable constellation, the only other possibilities available would be the narrow nose silhouette or tail silhouette of an aircraft, as a radar scatter cross-section.

It has in no way been established that the area of origin of the multi-tone effect must be localised in the troposphere. Observations at high aerial elevation do not unanimously exclude the upper atmosphere as a location of origin (especially the mesosphere and the E region in the ionosphere). An outcome of this kind, of course, would have a sensational character and would emphasise the scientific goals of amateur radio in lasting fashion.

5. SUMMARY

The multi-tone effect is a phenomenon which has so far been observed only by radio amateurs. An outside modulation, with an as yet unknown origin, is exerted on the transmission signal on the path of propagation. The widening of the spectrum goes along with a sometimes considerable error in the indication of the direction of reception. The occurrence can be observed almost daily.

No systematic pattern has yet been observed in the observation times, directions or widenings of the spectrum. Further experimental research appears unavoidable, in order to explain the phenomenon physically. Research of this nature could ideally be undertaken by beacon transmitters.

Of course, from practical experience, the author must qualify this by saying that inconsiderate disregard for the range exclusively reserved for beacons by amateurs transmitting in frequency modulation in it leads to a continuous limitation of the observation possibilities, as continuous long-term observations can scarcely be carried out.

6. LITERATURE

(1) H.J.Griem: (Untitled observation report) cq-DL, no. 9, 1976, p. 332

(2) H.J.Griem: Anomalous VHF Propagation cq-DL, no. 12, 1979, p. 577

(3) G.Hoch: Anomalous VHF Propagation cq-DL, no. 4, 1980, p. 195

(4) P.Pasteur: Anomalous VHF Propagation cq-DL, no. 6, 1980, p. 287

(5) G.Hoch: Anomalous VHF Propagation cq-DL, no. 10, 1980, p. 486

(6) V.Grassmann: Observation of the Multi-Tone Effect at Beacon Transmitter DLOPR 1982, unpublished

(7) V.Grassmann: The Multi-Tone Effect Dubus, no. 1, 1986, pp. 89 -90

(8) F.W.Bode: Personal Report, 1987

Dipl.-Ing. Fritz Hanf

New developments in High-Power Travelling Wave Tube designs

A number of high-powered Travelling Wave Tubes (TWTs) were recently developed for up-link satellite operation. The bands in use for this kind of operation are the following: 6 GHz, 14 GHz and 30 GHz. Unfortunately, these do not quite include the amateur bands, however, the techniques used to obtain the necessary power levels might of course be used in the future to manufacture TWTs useful to radio amateurs.

The main limiting factor for a travelling wave tube's output power is that the RF dissipation and the energy of the spent electron beam cause a great deal of heating effect. This heat must be conducted away from the Helix by means of electrically insulating materials to the main heat sinking medium. The insulators generally available up to now have not necessarily good conductors of heat and can also be susceptible to evaporation by the extremely hot Helix.

By means of new materials with good heat-conducting characteristics and the use of new technologies it has been possible to reduce the operating temperature of the Helix and thus increase the possible RF power output quite considerably.

Shrink technology has been applied to the type of TWT discussed here (YH1421). The Helix is constructed from Tungsten and is inserted, together with three Boron Nitride rods, into the vacuum envelope (Fig.1), which has been heated up to 770°C. The entire structure is held in position by the compression formed by the reduction in diameter of the envelope (shrinking) when it cools down.

Instead of glass, the envelope is formed of airtight soldered pole-pieces and non-magnetic spacers. The central opening that holds the Helix system is polished and honed with a great deal of precision. The quality of the heat transmission between the Helix and the envelope depends on the compacting pressure,

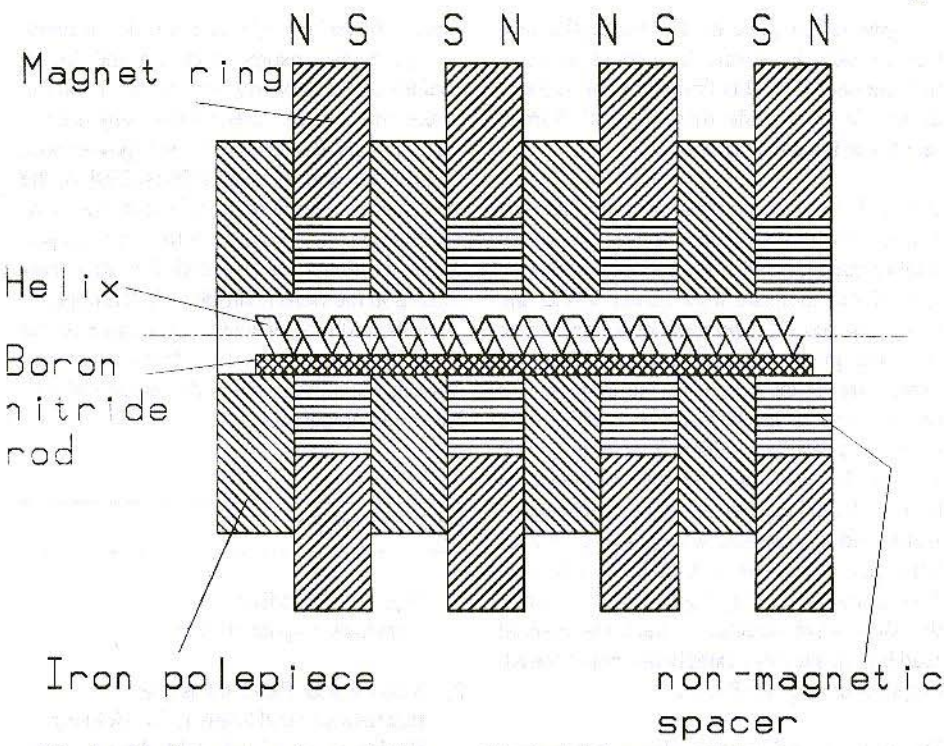

Fig.1a: Basic construction technique used in the high-power TWT

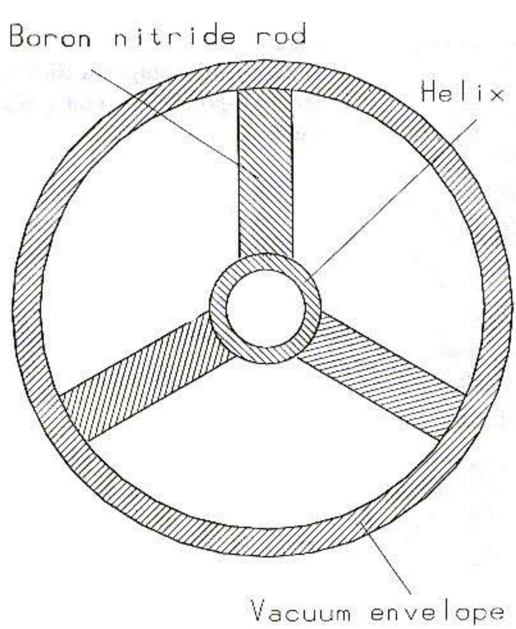

Fig.2:
Cross-sectional view of the Helix cavity

the greater the pressure the better the heat transmission. However, the amount of pressure that can be used is limited by the strength of the Boron Nitride rods. Typical thermal resistance is a 3 to 5°C/Watt.

It is still necessary to consider the thermal conduction from the vacuum envelope to the cooling medium (which is the air, although a few of the Siemens high power TWTs are water cooled). The thermal resistance of an iron pole-piece corresponds to 1°C/Watt per centimetre of the length of the system. If a copper core is inserted in the middle of a pole-piece and is soldered to the cooled waveguide, then the thermal resistance is halved. A total thermal resistance between the Helix and the cooled waveguide of 3.5°C/Watt per centimetre can thus be achieved. This technique is only applied in that part of the slow-wave structure where the thermal load is at its greatest, namely in front of the RF output coupling (see Fig.2).

Using this technique a number of tubes have been built with RF output powers of up to 900 Watts. The technologies used for the electron-gun, permanent magnet focusing and the sir cooling of the slow-wave structure are state-of-the-art for these tubes, which being used in earth stations. Because of the high power gain, 50 to 60dB, and to avoid self-oscillation, the slow-wave structure of the tube is divided into three segments; input, centre and output. These sections are isolated by attenuator regions in the Boron Nitride rods. To improve linearity and tube efficiency, the taper of the Helix is matched to the election velocity towards the output, which decreases with the RF circuit modulation.

REFERENCES

1) Dipl.-Ing. Fritz Hanf
Siemens Components 6/89

2) Siemens AG, Bereich Passive
Bauelemente und Rohren, Entwicklung
Hochleistungs-Wanderfeldrohren,
Munchen.

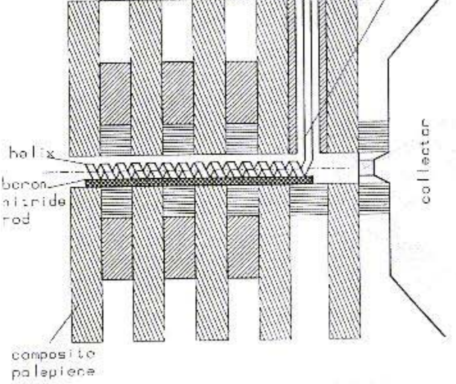

Fig.2:
Details of the output section of the high-power Travelling Wave Tube

Robert E. Lentz DL3WR

Digitally Transmitted Weather Satellite Images

Now that VHF Communications and our readers - and, indeed, a large part of the radio amateur world - have been familiar with the reception and the displaying of weather satellite images for over a decade, it istime to begin a new chapter.

So far, we have been involved exclusively with images transferred by analogue systems (FM/AM) from the polar orbit satellites (NOAA and Meteor), using the APT process, and from the geostationary weather satellites (Meteosat, GOES, GMS) in WEFAX format. Yet, with the exception of the Meteor range, all weather satellites also transmit their images in digital form, which has various advantages, which I shall come back to later. Digital transmissions are, in principle, also accessible to all - so why shouldn't we make use of them?

As a general comment, we can say that digital image transmission has two main advantages:

- **The complete geometrical resolution is made available.**

- **The radiometric data can be calibrated, which, among other things, makes it possible to measure the surface temperatures on an infra-red image**

However, when it comes to the detailed picture, the differences between the satellites are considerable, so that I shall proceed to deal with them all in turn.

1. SATELLITES WITH DIGITAL WEATHER IMAGES

Fig.1 shows the global weather satellite system. Of these satellites we are not interested in the Meteor range, for the aforementioned reasons. Nor does Insat concern us, because it is not generally accessible. Our curiosity extends to all the others.

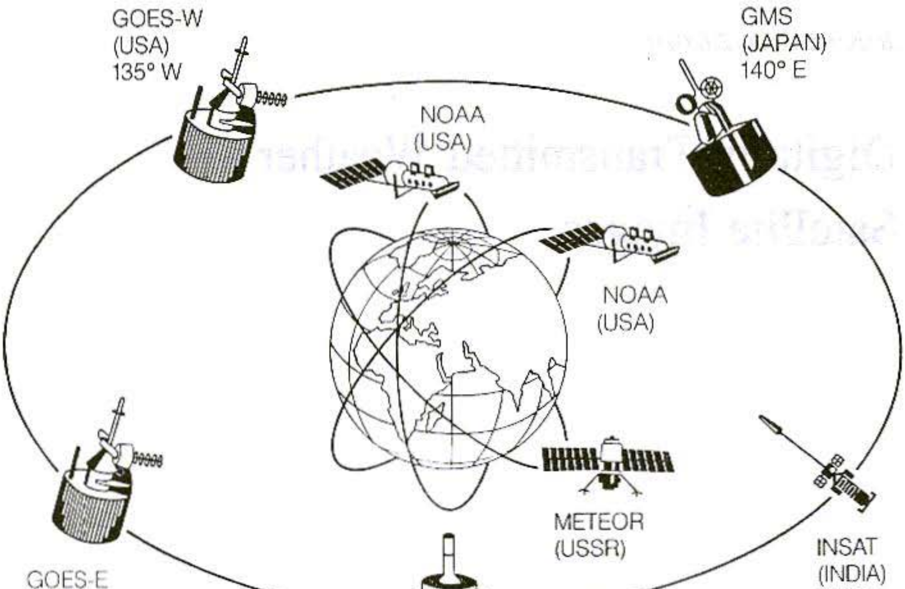

Fig.1: The Global System of Weather Satellites

1.1 METEOSAT

Meteosat, the geostationary weather satellite for Europe and Africa, transmits images in a digital format on 1694.500 MHz. These are not the so-called raw data, but the images originating in the big ESOC computer in Darmstadt. In this PDUS (primary data user station) mode, as with the WEFAX images, the satellite is thus used as a transponder for the distribution of the processed images. There are three different formats:

- A = Total image of entire Earth surface visible from Meteosat
- B = Image segment of Europe (somewhat wider than WEFAX D2)
- X = North and South America (received from GOES-E via Lannion)

The three spectrum channels of the radiometer are naturally the same as those we know from the WEFAX images:

- *VIS = Images in visible light. Resolution at sub-satellite point - 2.5km.
- *IR = Images in thermal infra-red (10.5 - 12.5um). Resolution at best 5km.
- *WV = IR images (5.7 - 7.1um.), which show the water vapour in the atmosphere. Resolution at best 5km.

The formats are transmitted at specific times according to a plan, the dissemination schedule, sometimes using only one spectrum channel (for example AI = total image in thermal IR, or AV = total image in visible light), but sometimes also using two, or all three, spectrum channels nested one inside another (e.g: BIW = Europe in two IR channels, or BIVW = Europe in all three channels). So you must consult the schedule to find out what is being transmitted. As for the transmission times, all "Admin Messages" can be received via the WEFAX program.

Depending on the number of pixels and spectrum channels (1, 2 or 3), the image transmissions last for very different periods of time. And the amounts of data which have to be processed vary just as much. With Meteosat, 8 bits are coded from each pixel, and the total image consists of 5,000 x 5,000 pixels (VIS) or 2,500 x 2,500 pixels (IR and WV). Anyone can work out what that is in bits or bytes. It is therefore normal for small PDUS installations to store only the image segments and spectrum channels desired, and to "throw away" the remaining data as soon as it is received.

That's enough explanation of the Meteosat-PDUS system. Anyone wishing to write software to process the PDUS images should obtain a copy of "Meteosat High-Resolution Image Dissemination" from the ESA (1).

So what benefits can be obtained from receiving PDUS images - apart from the technical challenge? In PDUS mode, you yourself program the image segment you wish to receive, and the spectrum channel. By selection of the segment and/or "zooming", any area desired can easily be displayed at the maximum possible geometric resolution. The values referred to (2.5 or 5km.), however, are obtained only at the point beneath the satellite, i.e: in the Gulf of Guinea. The greater the geographical width of the selected area, the more oblique the view and the lower the resolution. True, you can stretch the image in the North-South direction using a simple mathematical operation, so that it looks "natural", but that doesn't make the resolution any better.

To give an idea of the possible resolution: the CO2 and CO3 WEFAX image segments have practically the maximum possible resolution. The only reason why it can not be made use of in many SDUS (secondary data user station) installations is because the demodulators and filters are not optimal.

Now, of course, a weather satellite is not there to show the landscape in as much detail as possible, although that is especially exciting to interested lay people. Of much greater importance is the number of shades of grey 8 bit = 256 stages, means very fine distinctions can be made between high clouds, low clouds and mist over land or water or ice - provided that the information content of the satellite data flow does not go down to only 4 or 6 bits due to shrinkage of the image display, and is not lost through absurd colours.

One fascinating thing about the PDUS images is that it is possible to measure the temperatures. On the IR image, you use the cursor to select a point on the image, and the software converts the gray scale value into a temperature by means of an algorithm and a table. The first time I had the chance to do this, in the mid-80's, I measured the surface temperature of the sea around the island of Crete a few days before my holidays, and was then able to look forward to snorkelling in 24 to 27?C, and the bath thermometer then confirmed that these temperatures were correct.

But since the IR transparency of the atmosphere between the surface point and the satellite fluctuates, and the IR sensor is variable, the calibration values and correction factors transmitted with the data flow must be taken into account. Obtaining reliable temperature values thus requires a certain amount of effort.

1.2 GOES and GMS

The other two geostationary satellites transmit digitally, but I intend to deal with them very briefly, as they play no role in Europe.

Both transmit their S-VISSR service on 1687.1 MHz. Here we are speaking of the original digital image data from the instrument referred to as the VISSR (visible and infra-red spin scan radiometer), which are stretched so that the bit rate is lower than that for the raw data.

However, for GOES it is still over 2 Mb/s., so that aerials with a diameter of 4 to 5m are needed for reception. The Japanese GMS needs almost the entire aerial diameter, although its S-VISSR bit rate amounts to only 660 kb/s.

So, I hope readers in Australia will pardon me if I lay the emphasis more on the NOAA-HRPT images, which can be received equally well anywhere on Earth.

1.3 NOAA and FengYun

The weather satellites of the NOAA range circle the Earth at a height of at least 800km in sun-synchronous orbits (roughly over the Poles). Their radiometers scan the Earth's surface beneath them strip by strip, and sensors in five different spectrum ranges convert the radiation reflected from the Earth into electrical signals, which are then digitised 10 bits deep. The data from the five channels are nested into each other line by line and packed into packages (frames) with a synchronisation word at the beginning. The time, identification signal, telemetry data and measurement readings from other instruments (TIP = TIROS Information Processor) are then stored in each package, as shown in Fig.2 (3). This provides a continuous data flow at 665.4 kb/s. There is always one image line in five spectrum channels per frame in quasi-real time.

All channels have the same geometrical resolution of 1.1km in the centre of the image. To the right and left, the images are noticeably compressed, due to the curvature of the Earth, at least in the outside third. A transmitter in the SHF range modulates the flow of digital data. The frequecies are:

1698.0 MHz for NOAA-10 and NOAA-12
or
1707.0 MHz for NOAA-9 and NOAA-11.

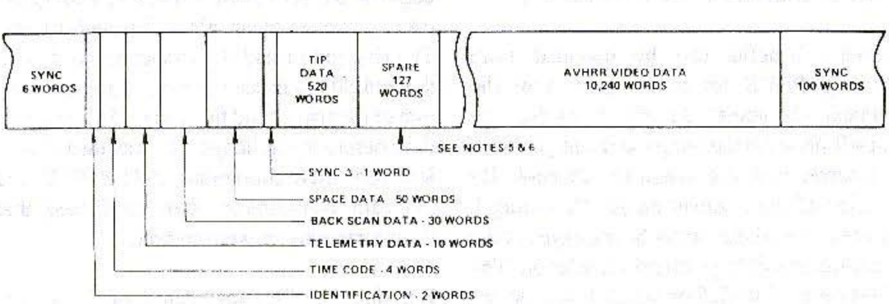

Fig.2: A NOAA-HRPT Frame

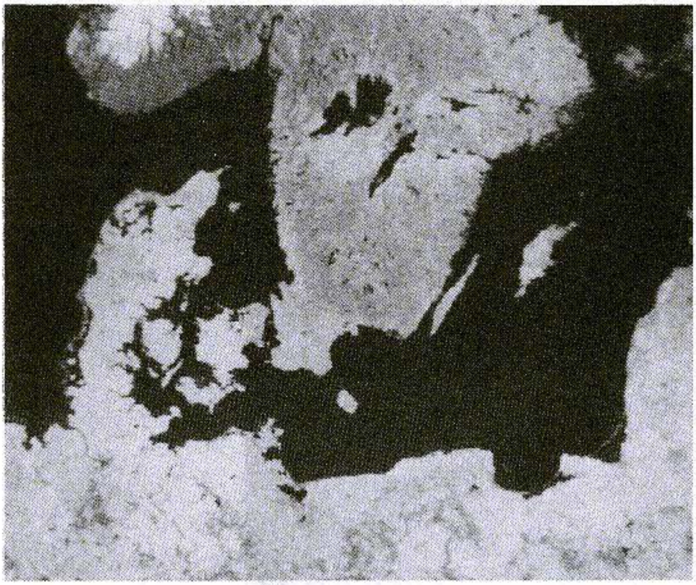

Fig.3:
The NOAA-HRPT image segment shows part of the North Sea and Baltic Sea and the last snow on Norway's mountains

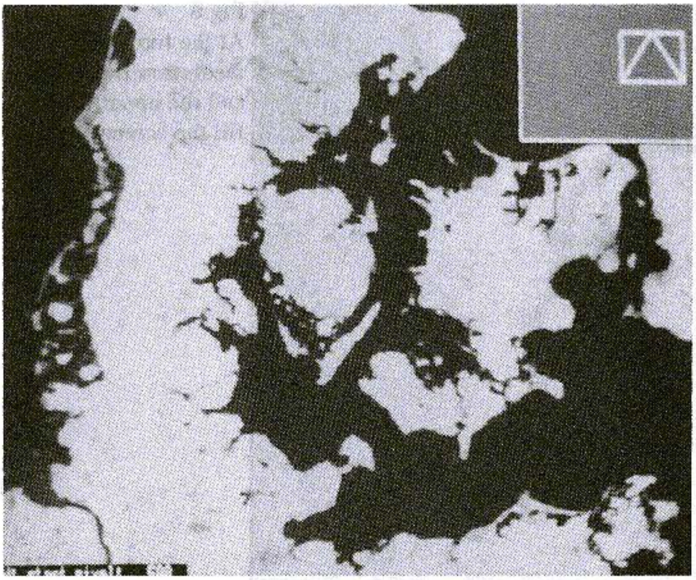

Fig.4:
The location and size of the image segment adjusted using zooming and displacement can be seen in the top right-hand corner

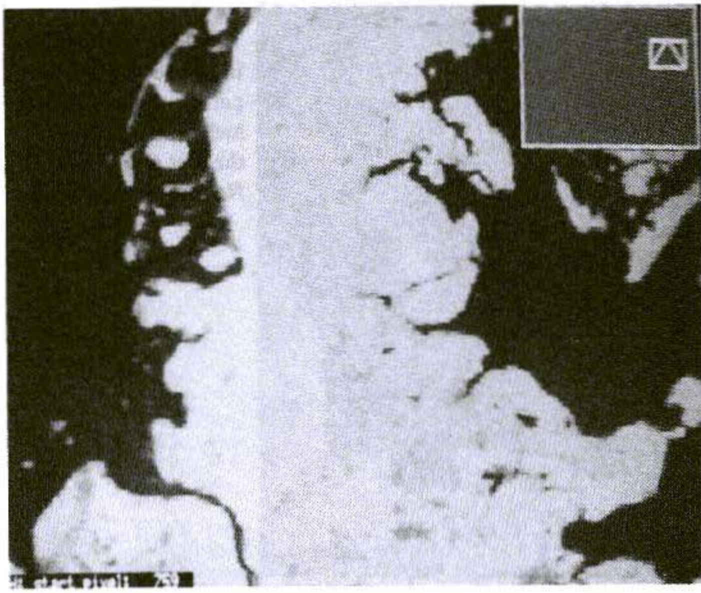

Fig.5:
Further enlargement and displacement of the segment causes Schleswig-Holstein to come into the image and fill the screen

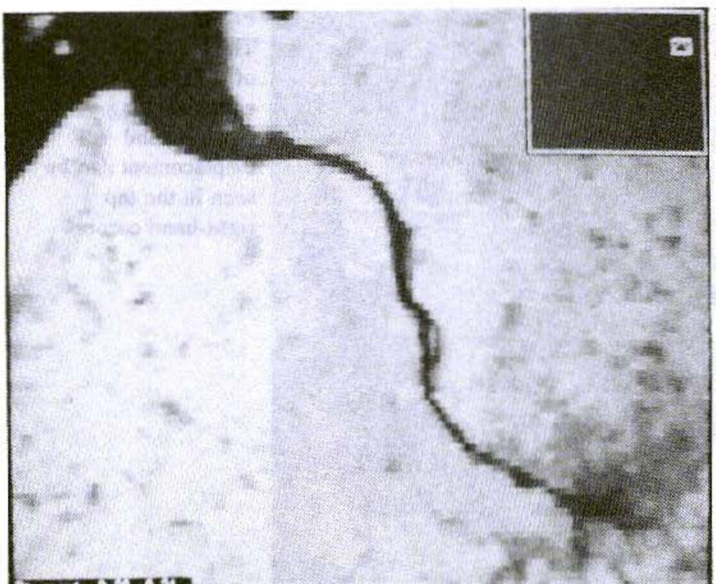

Fig.6
At the limit of resolution Hamburg and the upper Elbe fill the screen

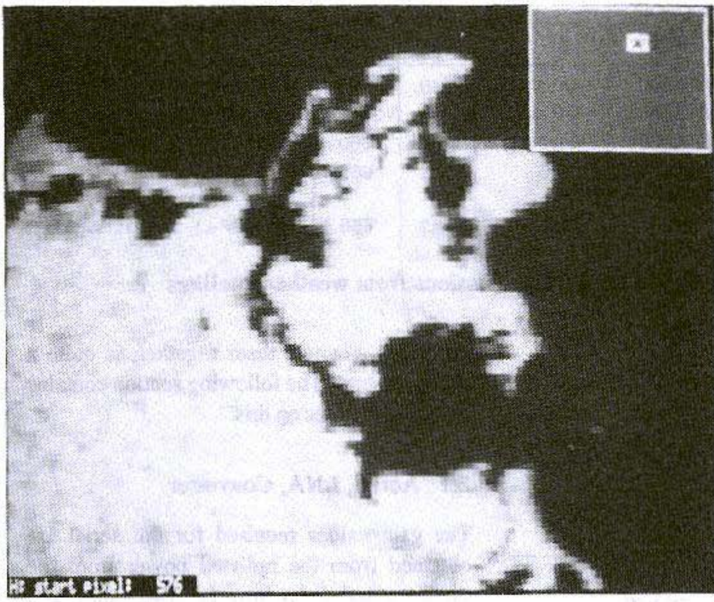

Fig.7: The limit of useful enlargement is reached when the individual pixels become clearly discernable

For analogue picture transmission (APT) in the VHF range, two spectrum channels are selected - usually one in the visible and one in the thermal IR - corrected in the outer areas (to balance out the curvature of the Earth somewhat) and then D/A converted.

In September, 1990, the People's Republic of China launched its second weather satellite in the FengYun range, known as FY-1B, into an orbit similar to one of the NOAA orbits (we reported the launch). The photography and image transmission represented a direct copy of the NOAA process, so that FY-1B images can be processed using the HRPT equipment. The transmission frequency was initially 1695.5 MHz, and was switched to 1704.5 MHz following a protest by the ESA. The ample width of the HRPT signal spectrum from FY-1B was in fact interfering with Meteosat's 1694.5 MHz frequency. FY-1B has been shut down since the beginning of 1991, after a malfunction set the satellite in uncontrolled motion. During the months in which it operated, it supplied excellent images.

I took the following screen photos using my DSP computer. They show how many details can be recognised from a good NOAA-HRPT image. Fig's.3 - 7 were obtained by means of continually zooming further and further, from the same stored image. Top right shows where the segment is located in the overall image and how big it is. The enlarging process reaches its limit when the pixels become clearly recognisable (Fig's.6 and 7).

All that commercial software can bring forth from the five spectrum channels of the NOAA-HRPT image data can not even be hinted at here. There are applications for it in almost all the natural sciences.

Satellite	Frequency MHz	Polarisation	EIRP dBm	Bitrate kb/s	Modulation	Index rad
METEOSAT	1694,500	linear (H)	49	166,6	PSK (SP-L)	1,2
GOES	1687,100	linear	54	2111,3	PSK (NRZ-S)	1,6
GMS	1687,100	linear	57	660	PSK (NRZ-M)	1,6
NOAA	1698,0 1707,0	RHC	39	665,4	PSK (SP-L)	1,2
FY-1B	1704,5 1695,5	RHC	39	665,4	PSK (SP-L)	1,2

Table 1: Data from digital image transmissions from weather satellites

1.4 Signal characteristics

To conclude this expedition through the weather satellites using digital transmission, I want to summarise their most important characteristics in Table 1.

2. RECEPTION EQUIPMENT

Irrespective of which of the satellites under discussion is to be received, the equipment always consists of the following components:

1) Aerial (for reception of orbiting satellites automatic aerial tracking is also required)
2) Aerial amplifier (LNA)
3) ConverterReceiver with PM demodulator
4) Bit synchroniser
5) Computer interface
6) Image computer with software

An outline circuit diagram would be superfluous with a "straight line circuit" of this kind. How you lay these components out and, if necessary, connect them together, is quite a different story. The following section contains basic instructions on this.

2.1 Aerial, LNA, Converter

The gain values required for the aerial are obtained from the radiated power from the satellites and from how far away they are, using a distance-budget calculation. For amateur applications, you can reckon without the worst case values, because the images received certainly do not all have to be free from faults under all circumstances, and because we can also actually "rotate" somewhat at specific points of the installation.

Table 2 therefore contains two gain values: one set are those from the literature from the satellite operators and the others - as far as is known - are the values determined in practical use by amateurs. The values listed in the amateur column for the minimum aerial gain required presuppose aerial amplifiers with a noise factor in accordance with the "state of the art"; for example, the LNA described by YT3MV in (4). When I received Meteosat

Satellite	Aerial gain professional	Aerial gain amateur
METEOSAT-PDUS	30 dB	26 dB
GOES S-VISSR	36 dB	
GMS S-VISSR	33 dB	
NOAA HRPT	27 dB	22 dB
FY-1B HRPT	27 dB	22 dB

Table 2: Aerial gain required for reception of digital image weather satellite transmissions

PDUS a few years ago, a 1.8m diameter was still insufficient. With the LNA value referred to, a diameter of 1.2m can be enough in certain circumstances! Correspondingly, the minimum diameter of an aerial for NOAA HRPT can today be 0.9m, whereas earlier 1.2m were necessary. So, perhaps I have made it clear that only parabolic antennae can be considered, and I have also referred to the optimal amateur LNA at the moment.

The converter has the task of converting SHF to VHF, 70 MHz, for example, can be considered as the IF. The amplification required is based on the cable attenuation and the receiver sensitivity. The phase noise of the converter oscillator is important. Over indulgence here means the aerial sizes referred to above are no longer sufficient.

2.2 Aerial tracking

It is certainly clear that the aerial must automatically track the pole-orbiting satellites. With the gain values provided, the aperture angle of the beam lobe is certainly very small, so that great demands are made on the rotors. In professional installations, the aerial tracking equipment is therefore a factor which is decisive for quality and price. Amateurs, on the other hand, can use the "satellite rotor system" from the normal amateur radio range. For some years I have used a KR-5600 B, which turns a 1.2m parabola and two small crossed Yagi's. Whilst initially it was merely calibrating the starting positions that caused problems, so much play has since developed that the antenna lobe goes past the signal maximum every time one motor, or both motors, is or are briefly switched on (by the controlling computer), and then levels out as best it may. So it's time for a replacement.

Nowadays, computer programs for automatic tracking, using the Kepler data and clock time, are like the sands of the sea, and the required interface circuits between the computer and the rotor control equipment are also on the market in sufficient numbers. I use the DSP computer publicised by YT3MV, with the associated interface and Track software (5), (6). This combination has the advantage that the aerial tracking is going on in the background, so that the computer itself can be used simultaneously for processing and displaying the data. I shall go into this in greater detail later.

2.3 Receivers, Pm De-modulators

The (IF) receiver must have a band width matched to the signal, such as AGC, so that no restriction arises and an S-meter can be operated. One of its oscillators must be in a phase-locked loop, so that the signal's doppler shift is eliminated. The same phase-locked loop can be used for phase demodulation. Here too great attention must be paid to the phase noise, so as not to make the modest signal worse than it is when received.

The phase demodulator supplies a signal which can be displayed on any oscilloscope: the "eye pattern" signal (Fig.8). If the timebase has been set in such a way that only two "eyes" are formed, you will understand how the description came about.

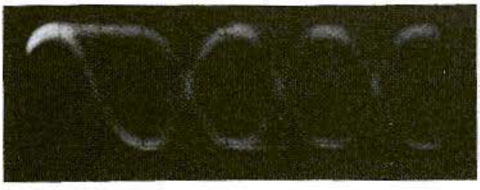

Fig.8: Eye pattern of a NOAA-HRPT signal

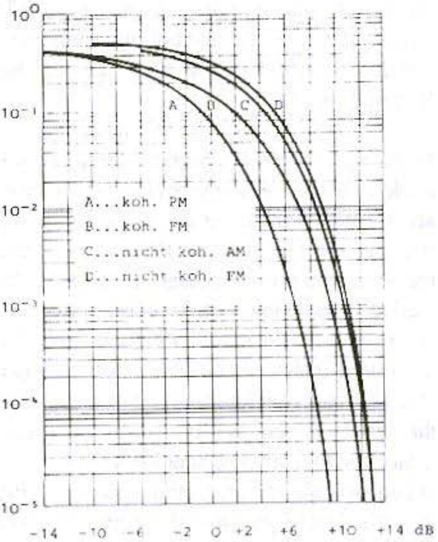

Fig.9: BER as a function of the bit energy per noise power density for two coherent and two non-coherent types of modulation. (koh.=coherent; nicht koh.= non-coherent)

This signal is still more or less noisy throughout, for up to now we have been working without any if's or but's in analogue technology, although we wish to receive a digital-coded signal. Only the bit-synchroniser, which we now turn to, will decide whether a bit represents a 1 or a 0.

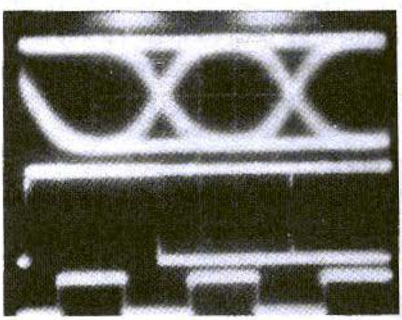

2.4. Bit and frame synchroniser

The eye pattern signal is fed into the bit synchroniser, which has two tasks. , Firstly together with a PLL, it must synchronise with the data flow and thus recover the bit timing. Secondly, the bit timing (665.4 kHz for NOAA HRPT) is used to scan each individual bit in a synchronous interrogation, for example in an S & H circuit, to determine whether a 0 or a 1 is present.

So we subsequently have available digital 1/0 sequences, plus the timing, with which the frame synchroniser can make a start. The 1/0 decisions of the bit synchroniser are more or less subject to error, because the eye pattern fed in is not free from noise. The yardstick for determining the error fraction is the bit error rate -BER for short. For digital data transmissions - irrespective of the information content of the transmission - there is a specific relationship between the BER and the signal/noise ratio for each individual type of modulation, Fig.9 gives an example.

It is remarkable that reducing the signal-to-noise ratio by a single dB immediately makes the BER a whole order of magnitude worse. The measure of a bit synchroniser is thus how close it can come to the theoretically possible BER in practical operation with noisy input signals.

As already stated, the bit synchroniser supplies the data and the timing (Fig.10).

Fig:10:
Simultanous representation of input and output signals of a bit-synchroniser;
top: eye pattern;
centre: data;
bottom: timing

The frame synchroniser has the job of fishing the "synchronisation word" out of the data flow. The synchronisation word is an unmistakable pattern, thought up by mathematicians, and made from ones and zeroes, which stands at a specific point in each frame - usually at the beginning. In our case, it tells the image computer when an image line begins.

The Meteosat PDUS synchronisation word is 24 bits long:

MSB 00000101 00001100 11011111

The NOAA-HRPT synchronisation word is 60 bits long:

MSB 1010000100 0101101111 1101011100
0110011101 1000001111 0010010101

In the simplest case, the frame synchroniser consists of a shift register of the same length as the synchronisation word, through which the data coming from the bit synchroniser can be pushed using the relevant timing. A "pyramid" made from hard-wired grids is waiting for the synchronisation pattern at the parallel outputs. Whenever the pattern appears, the tip of the pyramid emits a pulse, the so-called synchronisation pulse. All signals required now become available for each image computer:

1) serial data
2) relevant timing
3) synchronisation pulse.

Since the frame synchroniser functions in a purely digital mode, it seems reasonable to copy its function in the image computer by means of software and thus economise a little on hardware.

You can find a detailed construction proposal for a Meteosat PDUS in (2). This is a suggestion which came from the University of Dundee in the second half of the seventies.

3.
IMAGE PROCESSING AND DISPLAY

Professional weather satellite reception installations use computers of the work-station class to process and display images. Here there is sufficient memory space and computing capacity for even the most complicated evaluations, and a large high-resolution monitor and hard copy colour equipment display the results to the human eye. Amateurs in several continents are at present mainly grabbing the nearest PC. These are becoming more and more capable.

The future of image processing in the lower professional range and in the amateur range undoubtedly belongs to the PC's, and we are waiting in suspense to see who can be the first to offer a throughput system combining hardware and software and satisfying the sophisticated demands on it. Cautious reports in various periodicals indicate that market tests are already being carried out, even if no throughput technology is available as yet. The main thing lacking is good aerial tracking equipment which is also reasonably priced.

One possibility, available immediately, is the DSP computer already mentioned from Matjaz Vidmar, YT3MV (see literature reference (6)). The images in this article were plotted and processed using his HRPTA software (6).

It is an experimental program, which will be developed further. It already has the capability for zooming, positive/negative display, altering the shade of grey pitch, North/South reversal, distortion correction and, last but not least, gridding. Here the appropriate segment

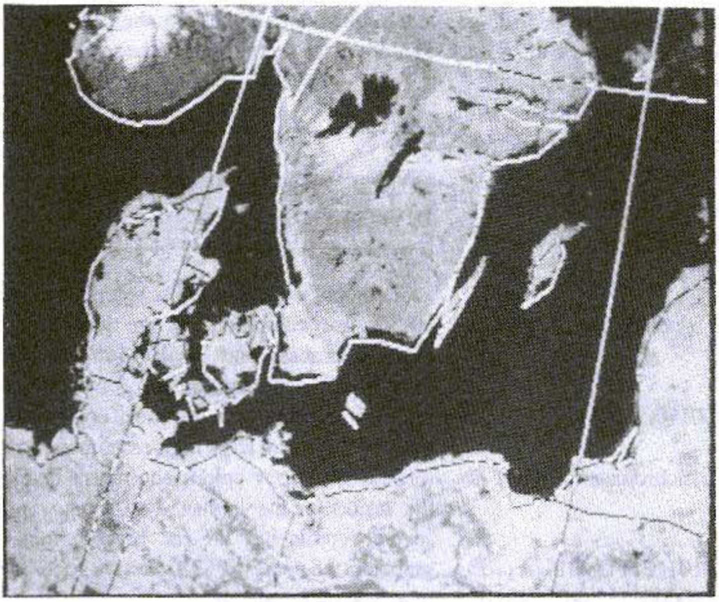

Fig.11: The same image segment as in Fig.3, but with reduced brightness, so that the land stands out more than the sea, and not the other way around - also with gridding overlay

of the weather image is superimposed from a data file on a (still somewhat approximate) outline of Europe, together with a co-ordinate network and the political borders. Since this must be done absolutely theoretically, using Kepler data and clock times, every discrepancy between the calculated orbit and the actual orbit of the satellites appears directly in the image. Gridding is consequently a check on the quality of the aerial's tracking. The example in Fig.11 shows the countries around the Western Baltic, and there is a very good match for Denmark with a gridding overlay.

Interested readers are welcome to contact the Editor with suggestions and queries.

4. LITERATURE

(1) ESA: Meteosat High-Resolution Image Dissemination

(2) ESA: A Meteosat Primary Data User Station

(3) NOAA: Technical Memorandum, NESS 95

(4) M.Vidmar YT3MV: A very Low-Noise Aerial Amplifier for the L-band
VHF Communications, 2/92 pp. 90 - 96

(5) M.Vidmar YT3MV: Digital Signal Processing Techniques for Radio Amateurs; Part 4: Amateur Radio Software for DSP Computer
VHF Communications 3/89 pp. 130 - 137

(6) M.Vidmar YT3MV: DSP Computer Update no. 1
VHF Communications, 3/91 pp. 147 - 157

Jim Toon G0FNH

10 GHz ATV The Easy Way
Part-4

Many people seem to think that constructing a 10 GHz amateur television station is hard to do. However, from the previous instalments of this series (1/91, 2/91 & 4/91) it can be seen that it is very easy to accomplish. However, having introduced a very simple system, let us see if we can improve the system. One improvement is to use a longer horn than the Solfan one, and so with this in mind we will set about it. At the same time we will also discuss the manufacture of a novel 10 GHz dipole aerial; very useful for test purposes.

1. HORN AERIALS

1.1 So how does a Horn Aerial work?

When a horn aerial is excited by microwave energy it works in a similar way to a megaphone, in that it restricts the energy of the microwave radiation into a narrow path, thus reducing the tendency for spreading. This, therefore, increases the intensity of the radiation along a particular path, or beam.

It is this property of being able to focus microwave beams which makes the horn aerial so useful. The energy can be directed and therefore illuminate distant objects, or be transmitted to a distant receiver with the minimum of interference from nearby transmitters. It also allows the effective power and range to be increased because the power is concentrated into one useful beam.

2. CONSTRUCTING A 20dB HORN AERIAL

To make our 20dB horn all that is required is some 1/16 inch sheet copper or brass (or any other plate that you can solder). If a thickness

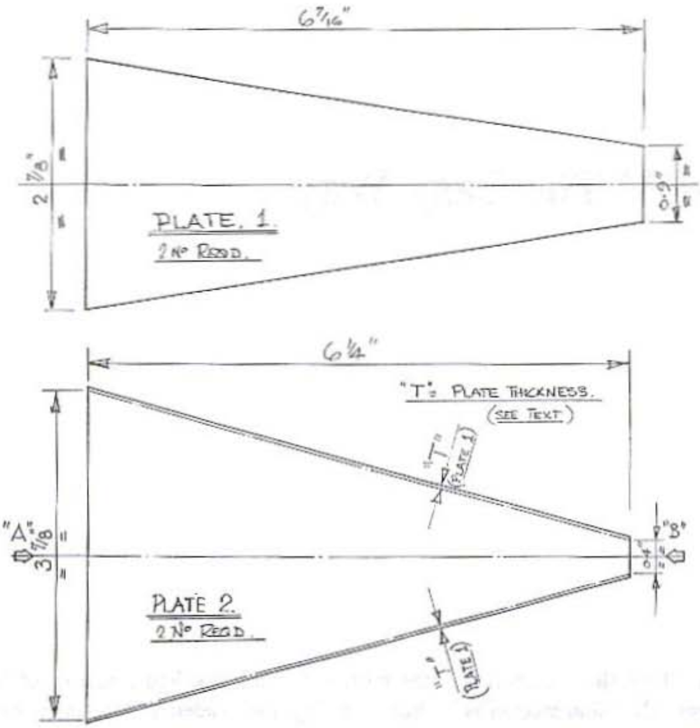

Fig.1: Details of plates for Horn Aerial

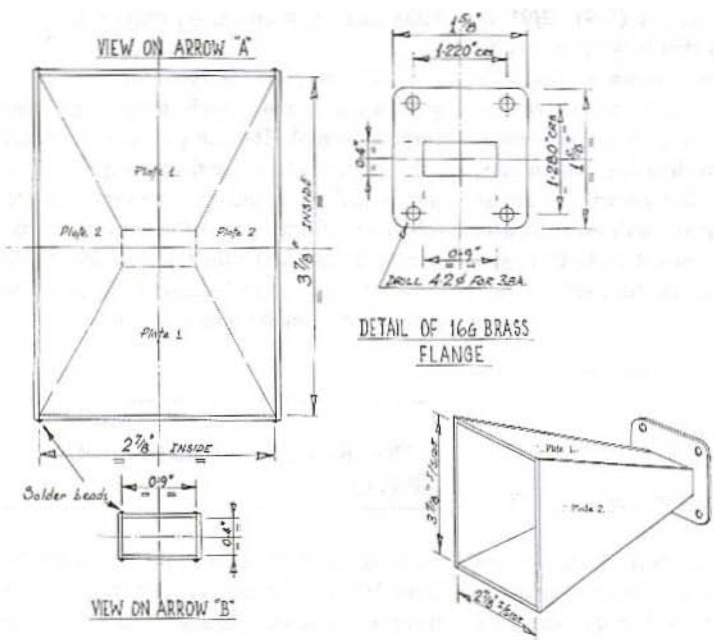

Fig.2: The Horn Aerial

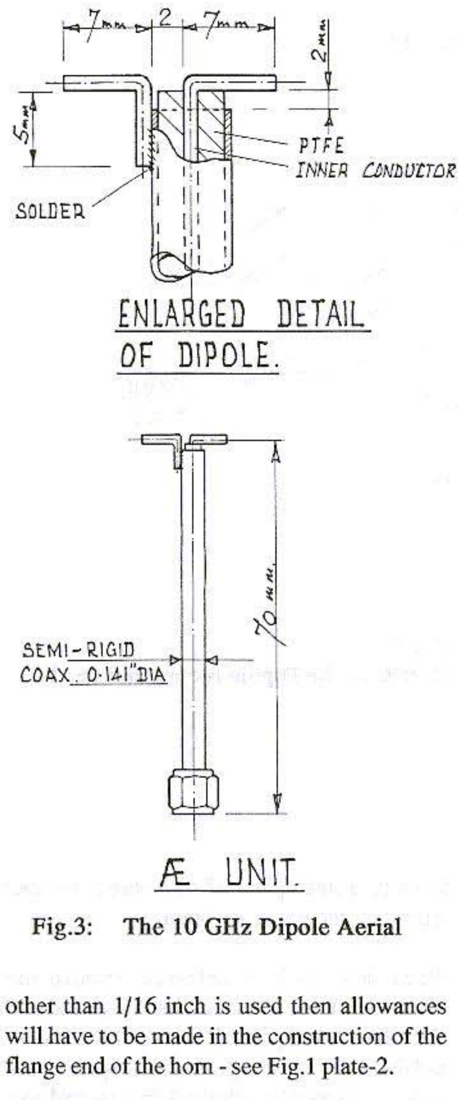

Fig.3: The 10 GHz Dipole Aerial

other than 1/16 inch is used then allowances will have to be made in the construction of the flange end of the horn - see Fig.1 plate-2.

Referring to Fig.1 plates 1 and 2 and Fig.2: Firstly, cut out the flange, ensuring that the middle section is 0.9 x 0.4 inches. Next, cut out the four sides sections making sure that they are nice and square. These four sections are then soldered together taking special care that they are square and that no solder gets on the insides.

I find that a very easy way of ensuring that the sides are all square is to cut a length of sheet plate about 6 inches long and about 1 inch wide folded lengthwise. This plate is clamped to two of the sides with small G-clamps and then the sides soldered together. When cold, move to the next side and so on.

Finally, the flange is soldered on nice and square, and all that is needed is a coat of spray paint, and that is it - a 20dB horn.

3. A 10 GHz DIPOLE!

Now we move on to the dipole shown in Fig's.3 and 4. For this project you will need some semi-rigid coaxial cable 0.141 inches in diameter. This can be be obtained at most rallies, usually with small SMA connectors on the ends. A piece around 90mm long is required. Also needed is one male SMA socket, one female SMA socket, a short length of waveguide 1.5 inches long with a small end plate and one flange.

Firstly, take the length of semi-rigid coaxial cable. Mark approximately 18mm down from one end and, with a sharp knife, score all the way round. Slowly bend the coax back and forth until the outer copper sheath breaks and then slide the sheath off to reveal the inner PTFE insulation. Mark 2mm up the revealed inner PTFE and strip it off the inner conductor, making sure that the inner conductor is not cut or scored. Save the PTFE as it is useful material!

Next, bend the inner conductor at right angles and measure from the bend 7mm and cut off the surplus. Retain the piece you have just cut off and bend it at right angles at about 5mm from one end and solder to the outer copper sheath of the semi-rigid coax as per Fig.3.

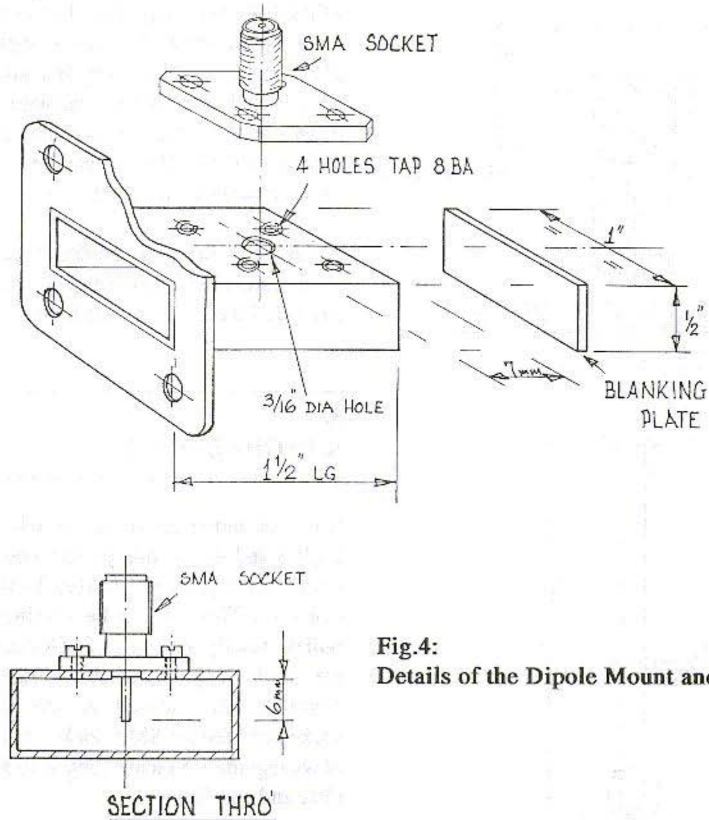

Fig.4: Details of the Dipole Mount and Feed

Mark off from the bend at 7mm and cut off the surplus. Now fit an SMA female socket (these solder very easily) and that's it.

Now we come to the waveguide transition as shown in Fig.4. Cut off a piece of waveguide 1.5 inches long and square up the ends. Mark from one end 7mm centrally on the waveguide and drill a 3/16 inch hole. Fit the SMA male socket into the hole and mark off the four holes shown in Fig.4 and drill and tap them 8BA. Fit the bolts and file flush on the inside of the waveguide. Ensure that the bolts do not protrude into the inside of the waveguide. The inner pin of the SMA socket DOES need to protrude 6mm into the waveguide. If the pin of the SMA socket is too short you will need to solder a small piece of wire onto it to make it protrude the necessary 6mm.

When this has been achieved, remove the SMA socket and solder on the flange and end plate, then spray paint. Refit the SMA socket and that's it. Don't forget that the dipole needs to be horizontally polarised in use and not vertical. I find this dipole very useful for setting up receivers.

NEVER FORGET: DO NOT LOOK INTO A HORN OR GET TOO CLOSE TO A MICROWAVE DIPOLE WHEN IN USE. EYES DO NOT LIKE MICROWAVES AT ALL!

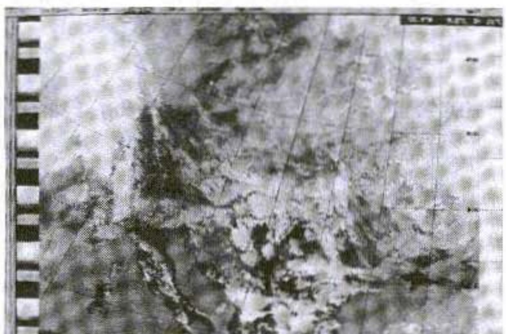

MATERIAL PRICE LIST OF EQUIPMENT

described in VHF COMMUNICATIONS

DJ8ES	FM ATV Receiver for the 23cm Band		Art.No.	Ed. 1/1991
Converter				
PCB	DJ8ES 001	double-sided	6347	DM 22.00
Components	DJ8ES 001		6348	DM 179.00
Kit	DJ8ES 001	complete	6349	DM 194.00
Digital Frequency Indicator				
PCB	DJ8ES 002	double-sided	6350	DM 19.80
Components	DJ8ES 002		6351	DM 94.00
Kit	DJ8ES 002	complete	6352	DM 110.00
IF Amplifier				
PCB	DJ8ES 003	double-sided	6353	DM 15.00
Components	DJ8ES 003		6354	DM 105.00
Kit	DJ8ES 003	complete	6355	DM 115.00
Demodulator				
PCB	DJ8ES 004	double-sided	6356	DM 19.00
Components	DJ8ES 004		6357	DM 136.00
Kit	DJ8ES 004	complete	6362	DM 150.00

DBINV	Digital Storage for the Spectrum Analyser	Art.No.	Ed. 3/1991
PCB	DB1NV EXper.1 (ed...)	6475	DM 29.90
PCB	DB1NV EXper.11 (solder spots 2.3 x 1mm)	6476	DM 29.90
PCB	DB1NV 010	6477	DM 44.00
Special	DB1NV 010, incl. programmed EPROM	6478	DM 276.00
Components:	DB1NV 010, EPROM only	10080	DM 44.00

DD2EK	Modifications of the FM-ATV TX DD2EK 002	Art.No.	Ed. 3/1991
PCB	DD2EK 002	6150	DM 28.00
Kit	DD2EK 002 without crystal but with MSA1104	6152/2	DM 145.00
Crystal	DD2EK 002 please give specified frequency	6153	DM 46.00

Post and packing minimum charges DM 14.00

The above items are all supplied by, and obtained from, UKW-Berichte in Germany.

To obtain supplies please contact your country representative for details of local prices and availability. Alternatively, you may order direct from UKW-Berichte or via KM Publications, whose addresses may be found on the inside front cover of this magazine.